ACS APPLIED MATERIALS & INTERFACES

Research Article

Cite This: ACS Appl. Mater. Interfaces 2018, 10, 16793−16801

www.acsami.org

Photoreversible Covalent Hydrogels for Soft-Matter Additive Manufacturing

Christopher P. Kabb,[†] Christopher S. O'Bryan,[‡] Christopher C. Deng,[†] Thomas E. Angelini,[‡,§,∥] and Brent S. Sumerlin*[,†]

[†]George & Josephine Butler Polymer Research Laboratory, Center for Macromolecular Science & Engineering, Department of Chemistry, [‡]Department of Mechanical and Aerospace Engineering, [§]J. Crayton Pruitt Family Department of Biomedical Engineering, and [∥]Institute for Cell and Regenerative Medicine, University of Florida, Gainesville, Florida 32611, United States

Supporting Information

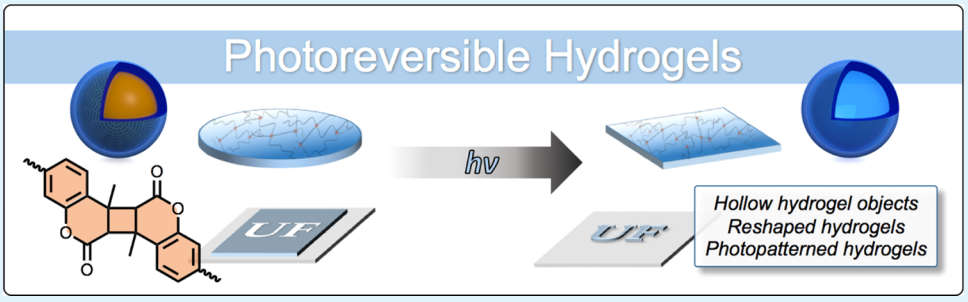

ABSTRACT: Reversible covalent chemistry provides access to robust materials with the ability to be degraded and reformed upon exposure to an appropriate stimulus. Photoresponsive units are attractive for this purpose, as the spatial and temporal application of light is easily controlled. Coumarin derivatives undergo a [2 + 2] cycloaddition upon exposure to long-wave UV irradiation (365 nm), and this process can be reversed using short-wave UV light (254 nm). Therefore, polymers cross-linked by coumarin groups are excellent candidates as reversible covalent gels. In this work, copolymerization of coumarin-containing monomers with the hydrophilic comonomer *N*,*N*-dimethylacrylamide yielded water-soluble, linear polymers that could be cured with long-wave UV light into free-standing hydrogels, even in the absence of a photoinitiator. Importantly, the gels were reverted back to soluble copolymers upon short-wave UV irradiation. This process could be cycled, allowing for recycling and remolding of the hydrogel into additional shapes. Further, this hydrogel can be imprinted with patterns through a mask-based, post-gelation photoetching method. Traditional limitations of this technique, such as the requirement for uniform etching in one direction, have been overcome by combining these materials with a soft-matter additive manufacturing methodology. In a representative application of this approach, we printed solid structures in which the interior coumarin-cross-linked gel is surrounded by a nondegradable gel. Upon exposure to short-wave UV irradiation, the coumarin-cross-linked gel was reverted to soluble prepolymers that were washed away to yield hollow hydrogel objects.

KEYWORDS: *Coumarin, hydrogel, reversible covalent, soft-matter additive manufacturing*

INTRODUCTION

Materials based upon reversible covalent chemistry[1] offer the strength of covalent bonds while retaining the reversible nature of noncovalent linkages. Incorporating such bonds within polymer networks provides robust materials that may be altered following their synthesis to induce changes in their physical and/or chemical properties. Reversible covalent linkages, such as photoresponsive cycloadducts,[2,3] Schiff bases,[4−6] Diels−Alder adducts,[7−10] disulfides,[11−13] and boronic esters,[14−17] have been exploited in the fabrication of functional materials,[18] imparting remendability and reprocessability to the materials they are contained within. Photosensitive reversible covalent moieties are of particular interest because of the inherent spatiotemporal control offered by light-driven reactions. In addition, the wavelength of light and luminous intensity can be carefully chosen to target desired reactions and/or reaction rates.

Functional groups which undergo photoreversible dimerization processes,[19] such as coumarins,[3,20−22] anthracene derivatives,[23] and pyrimidine bases,[24,25] provide an avenue toward reversible formation and photolytic cleavage of polymer networks. Coumarin derivatives have been used as cross-linking groups in polymeric materials because of the relatively mild conditions necessary for dimerization and the ability to undergo iterative cycloadditions/cycloreversions.[2,26−32] Under long-wave UV irradiation (365 nm), coumarins undergo a [2 + 2] cycloaddition to yield cyclobutane-linked dimers. Therefore, the installation of coumarin groups on a polymer backbone enables facile cross-linking through the formation of coumarin

Received: February 8, 2018
Accepted: April 20, 2018
Published: May 4, 2018

DOI: 10.1021/acsami.8b02441
ACS Appl. Mater. Interfaces 2018, 10, 16793−16801

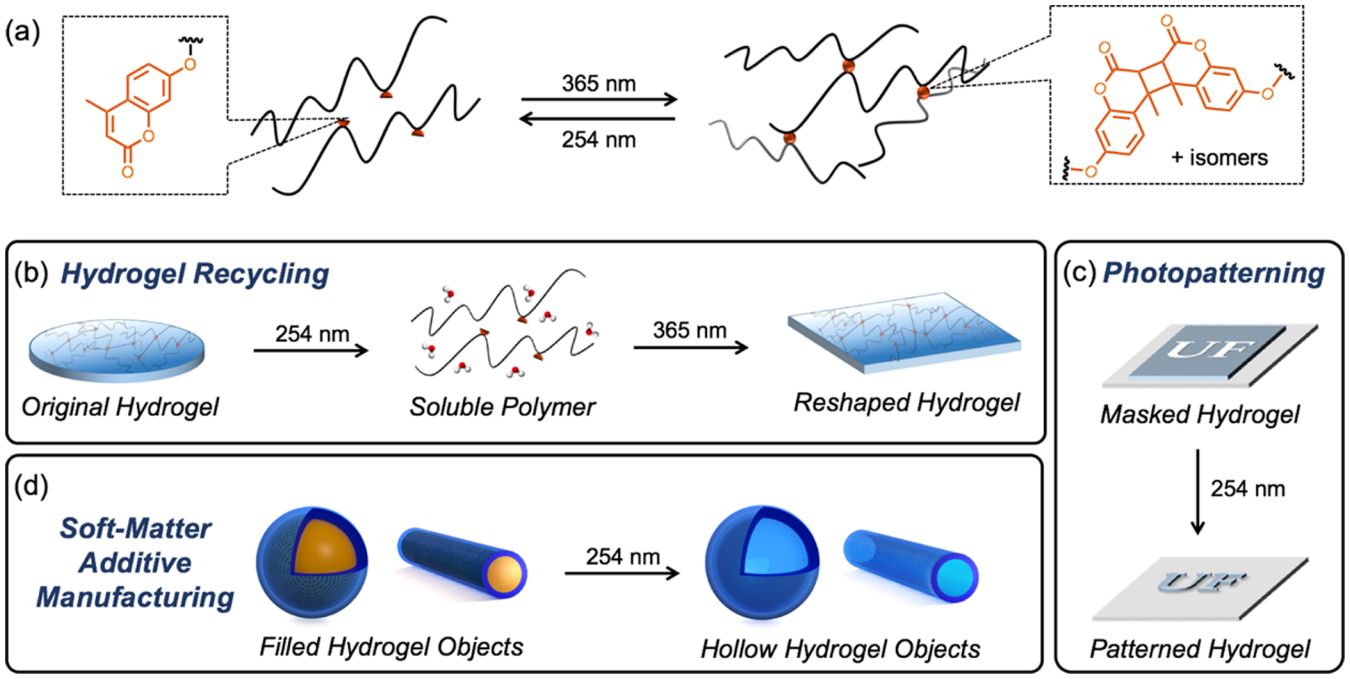

Figure 1. Routes to reversible covalent materials linked by photosensitive coumarin dimers. (a) Water-soluble copolymers containing pendent coumarin functionality can be reversibly cross-linked using UV light to generate photoreversible hydrogels. (b) Polymer hydrogels cross-linked by the dimerization of coumarin can be broken down to soluble polymers using 254 nm light, remolded, and cured into a hydrogel of a new shape. (c) Patterned hydrogels can be formed by irradiating a masked hydrogel with 254 nm light to reverse the unmasked areas. (d) Combining photodegradable hydrogels with nondegradable hydrogels via soft-matter additive manufacturing provides access to complex structures such as hollow hydrogel spheres and tubes.

dimers. For example, Yoshida and coworkers installed pendent coumarin functionality in a thermoresponsive poly(*N*-isopropylacrylamide) (PNIPAM) block of an ABA triblock copolymer.[33] Above the cloud point of the PNIPAM block, the polymers assembled into flower micelles, forming a physical network. After irradiating the hydrogel with long-wave UV light, dimerization of pendent coumarins formed a chemically cross-linked network, and the change in modulus led to a significantly altered behavior of encapsulated cells. When coumarin dimers are exposed to short-wave UV irradiation (254 nm), a cycloreversion reaction occurs, leading to partial recovery of the uncross-linked form.[34] This allows for cross-linking with long-wave UV radiation and reversion to soluble copolymers using short-wave UV light. Ling et al. demonstrated the efficient dimerization and retrocyclization of coumarins by using this reversibility as a means for self-healing of a polymeric film.[35] A poly(ethylene glycol) (PEG)-based polyurethane was prepared with a pendent coumarin in the repeat unit. A cross-linked film was cut and then repaired with successive irradiation with short-wave and long-wave UV light, displaying excellent healing of the damaged area. After three cut-heal cycles, tensile testing demonstrated that over half of the original mechanical strength was retained, suggesting efficient reversibility of the coumarin linkage.

Hydrogels, which are cross-linked polymer networks swollen by water, are of great interest in areas such as regenerative medicine because they often have low moduli, can encapsulate cells, and are generally straightforward to prepare.[36,37] Fabricating soft hydrogel materials with distinct shapes poses a challenge because of their proclivity to deform under their own weight before and after polymerizing.[38,39] Light can be used via a top-down approach (i.e., post-gelation modification) to further alter a uniform hydrogel through photochemical reactions after initial cross-linking, which is analogous to the processes traditionally used for the preparation of photoresists.[40] This may include polymerizable groups such as acrylates which can either undergo radical photopolymerization or thiol−ene reactions.[10,41−44] In other cases, incorporating photodegradable functional groups allows for ablation of areas exposed to the light source. For example, *o*-nitrobenzyl groups incorporated at the cross-linking points of a PEG network allowed for photomediated degradation of the irradiated area, generating channels which guided cell migration in the hydrogel.[45,46] Such examples pinpoint the precision with which patterns can be generated if the reactive functionalities and the light source are properly selected. Further, because mask-based photoablation uses light to selectively etch unmasked areas of the hydrogel, simultaneous and inexpensive processing of multiple samples is possible, often with simple and readily available equipment. Conversely, patterns can be incorporated during the fabrication of the hydrogel (i.e., bottom up), such as in layer-by-layer stereolithography,[47] in which each layer is cured sequentially and excess monomer is washed away between steps, making processing of multiple samples challenging and time-consuming. Often, limited complexity can be incorporated into the materials, and softer substrates suffer from excessive material sag. Alternatively, 3D printing a liquid ink into a sacrificial support medium that can be subsequently removed after curing of the printed object circumvents these issues.[48] One benefit of this technique is the ability to print the entire object as a liquid before curing, providing near-perfect adhesion between layers. As a consequence, complex structures made from hydrogels, silicone elastomers, and even cellular constructs have been printed into sacrificial support materials ranging from jammed granular microgels and polymer networks with reversible bonds to entangled polymer solutions and packed micelles.[49−55] However, significant challenges remain when removing the support medium from within small-bore perfusable tube networks and encapsulated structures.

DOI: 10.1021/acsami.8b02441
ACS Appl. Mater. Interfaces 2018, 10, 16793−16801

In this work, we employ the reversible dimerization of coumarin as a means of cross-linking latent prepolymers into hydrogels. We exploit the direct copolymerization of coumarin-containing monomers with a hydrophilic comonomer as a route to water-soluble copolymers with pendent coumarin functionality. The dimerization of coumarins in solvents with varying polarity has been studied, with high quantum yields observed in water.[56] Therefore, following cross-linking of the coumarin units and removal of the surrounding support medium, free-standing hydrogels could be obtained which, upon exposure to short-wave UV irradiation, can be degraded into soluble copolymers (Figure 1a). As a consequence, hydrogels may be prepared in one shape, degraded through retrocyclization to regenerate the soluble precursor polymer, and subsequently molded and cured into a new shape (Figure 1b). Furthermore, this dynamic reversibility provides a concise route to photopatterned hydrogels in the presence of a photomask. Under these conditions, only the areas not covered by the photomask will be affected by the light source, leaving a clear pattern imprinted in the hydrogel (Figure 1c). Finally, combining these reversible covalent hydrogels with soft-matter 3D-printing technology allows access to an endless number of more complex structures, such as hollow hydrogel spheres and tubular structures (Figure 1d). The application of coumarin-cross-linked hydrogels in a top-down approach, as well as their use as a degradable ink to assist in bottom-up additive manufacturing, highlights their versatility and tremendous potential in the production of sophisticated soft materials and 3D cell-culture scaffolds.

MATERIALS AND EXPERIMENTAL METHODS

Detailed synthetic procedures and methodological details are provided in the Supporting Information. Coumarin-containing copolymers were synthesized via radical copolymerization of *N*,*N*-dimethylacrylamide (DMA) with either an acrylic (7-(2-acryloyloxyethoxy)-4-methylcoumarin) or acrylamido (7-(2-acrylamidoethoxy)-4-methylcoumarin) monomer with coumarin functionality. The monomers were mixed at a desired molar ratio (99:1 or 95:5) in 1,4-dioxane, and polymerization was initiated thermally using azobisisobutyronitrile. Number-average molecular weights, weight-average molecular weights, and molar mass dispersities were measured using gel permeation chromatography equipped with multi-angle light scattering detection. Coumarin incorporation in the purified copolymers was measured using ^{1}H NMR spectroscopy in $CDCl_3$. All cyclization (using long-wave UV light) and retrocyclization (using short-wave UV light) were performed with commercially available lamps with emission centered around 365 nm (long-wave UV) or 254 nm (short-wave UV). Coumarin dimerization and retrocyclization kinetics were studied in aqueous solution by monitoring the change in absorbance at λ = 320 nm, corresponding to the consumption or reemergence of the vinyl group of the α,β-unsaturated ester, respectively.

Soft-matter additive manufacturing was performed using custom-built instruments described previously.[49] In short, three linear translational stages were used, with a fourth linear stage as a syringe pump. The stages were controlled with custom-written MATLAB scripts and trajectories. Prepolymer solutions were loaded into a glass syringe with a 26-gauge blunt dispensing needle and printed into a jammed microgel support medium (Ashland 980 carbomer prepared at 0.15 wt % polymer and neutral pH). The printed inks were cured into hydrogels using a UV flood curing lamp with an emission window of 320−390 nm. To print objects containing two disparate hydrogels, two separate dispensing syringes were used. The MATLAB scripts were written to accommodate interchanging the two syringes at appropriate points in the printing process.

RESULTS AND DISCUSSION

Copolymers containing coumarin functionality have been synthesized by a variety of methods, including polycondensation of A−A- and B−B-type monomers,[3,35,57] radical polymerization of vinyl monomers,[33,58,59] and post-polymerization incorporation of coumarin-containing molecules.[60,61] Our strategy for incorporation of pendent coumarins into hydrophilic copolymers was to directly copolymerize coumarin-containing vinyl monomers with a water-soluble comonomer. This allows for accurate control over the coumarin incorporation through variation of the comonomer feed ratio. Therefore, the polymers were produced via radical copolymerization of DMA with one of two coumarin-based vinyl monomers (Figure 2). The first, 7-(2-acryloyloxyethoxy)-4-methylcoumarin (CoumAc), was synthesized according to a previous report.[62] A second acrylamide-based monomer necessitated the use of a *boc*-protected bromoethylamine to install the acrylamide functionality. Following deprotection, the amino-terminated coumarin was acylated with acryloyl chloride to yield 7-(2-acrylamidoethoxy)-4-methylcoumarin (CoumAAm). The structures of the intermediates and monomers were confirmed using ^{1}H and ^{13}C NMR spectroscopy and electrospray ionization high-resolution mass spectrometry (Figures S1−S8). UV−vis spectra of both monomers displayed the characteristic maximum absorbance of the coumarin unit at 320 nm (Figures S9 and S10).

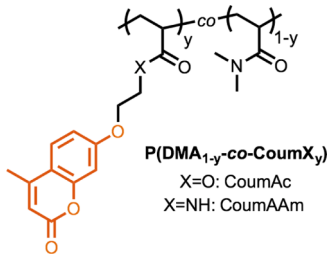

Figure 2. Structure of PDMA/coumarin copolymers. DMA and coumarin-containing monomers were copolymerized using conventional radical polymerization to yield water-soluble copolymers.

Initial copolymerizations were conducted with a molar ratio of $[DMA]_o/[CoumX]_o$ of 99:1. Reactions were carried out with a monomer concentration of 1.5 M in 1,4-dioxane at 70 °C. After 1 h, the viscosity of the solution drastically increased, and gel permeation chromatography with multi-angle light scattering detection (GPC-MALS) yielded molecular weights in the range of 100 kg mol^{-1} (Figure S11). After polymerization, the reaction mixture was dialyzed against deionized water to remove unreacted monomers and initiators, and the purified polymers were analyzed by ^{1}H NMR spectroscopy and Fourier transform infrared (FTIR) spectroscopy to identify the presence of coumarin functionality in the final copolymers (Figures S12−S16). For all polymers, NMR analysis indicated that the incorporation of coumarin units in the purified polymers closely matched the initial monomer feed ratio. Increasing the relative amount of the coumarin monomer to 5 mol % resulted in macroscopic gelation under the conditions described above, which is potentially attributed to either chain transfer to the vinylic methyl group of coumarin, or to polymerization directly through the coumarin vinyl group. This undesired result was suppressed by decreasing the monomer concentration to 0.5 M and lowering the polymerization temperature to 60 °C resulting in soluble copolymers with molecular weights in the range of 90−

DOI: 10.1021/acsami.8b02441
ACS Appl. Mater. Interfaces 2018, 10, 16793−16801

150 kg mol^{-1}, as determined by GPC-MALS. The results of typical copolymerizations are summarized in Table 1.

Table 1. Summary of DMA/Coumarin Copolymers

sample	y_{feed} [%][a]	$y_{copolymer}$ [%][b]	M_n [kg mol^{-1}][c]	M_w/M_n[c]
P(DMA$_{0.99}$-*co*-CoumAc$_{0.01}$)[d]	1	1	105	2.22
P(DMA$_{0.99}$-*co*-CoumAAm$_{0.01}$)[d]	1	1	100	3.07
P(DMA$_{0.95}$-*co*-CoumAc$_{0.05}$)[e]	5	6	156	2.23
P(DMA$_{0.95}$-*co*-CoumAAm$_{0.05}$)[e]	5	4	90.5	1.81

[a]Denotes the initial molar feed ratio of y_{feed} = [CoumX]$_o$/[CoumX + DMA]$_o$ × 100. [b]The incorporation of CoumX ($y_{copolymer}$) as measured from ^{1}H NMR spectroscopy of the purified copolymer. [c]Measured using GPC with multi-angle light scattering detection. [d][M]$_o$ = 1.5 M, T = 70 °C. [e][M]$_o$ = 0.5 M, T = 60 °C.

The solution dimerization/retrodimerization behavior of these copolymers was examined using UV−vis spectroscopy, as coumarin possesses a strong absorbance at 320 nm that diminishes upon dimerization. A dilute solution of P(DMA$_{0.95}$-*co*-CoumAc$_{0.05}$) (0.05 wt % in water) was prepared and exposed to 365 nm light. UV−vis spectra were recorded as a function of the irradiation time and, as expected, the absorbance at 320 nm decreased as the coumarin groups dimerized and conjugation was lost (Figure 3a). After 1 h, approximately 80% of coumarin moieties were in their dimeric form (Figure 3b). As the coumarin dimer can be reverted back to its monomeric form under short-wave irradiation, we postulated that recovery of the original prepolymer should be possible. Irradiation of the dimerized solution with 254 nm light led to a recovery of absorbance (Figure 3c), corresponding to cleavage of over 80% of coumarin dimers in 15 min (Figure 3d). Cycloreversion was not quantitative because of the establishment of an equilibrium between the forward and reverse reactions under short-wave UV irradiation.[63−65] When P(DMA$_{0.95}$-*co*-CoumAAm$_{0.05}$) was used in the same experiments, similar results were obtained (Figures S17 and S18).

The effect of the polymer concentration and coumarin content in the copolymer on the dimerization kinetics was also examined. First, dimerization of P(DMA$_{0.95}$-*co*-CoumAc$_{0.05}$) at 0.02 and

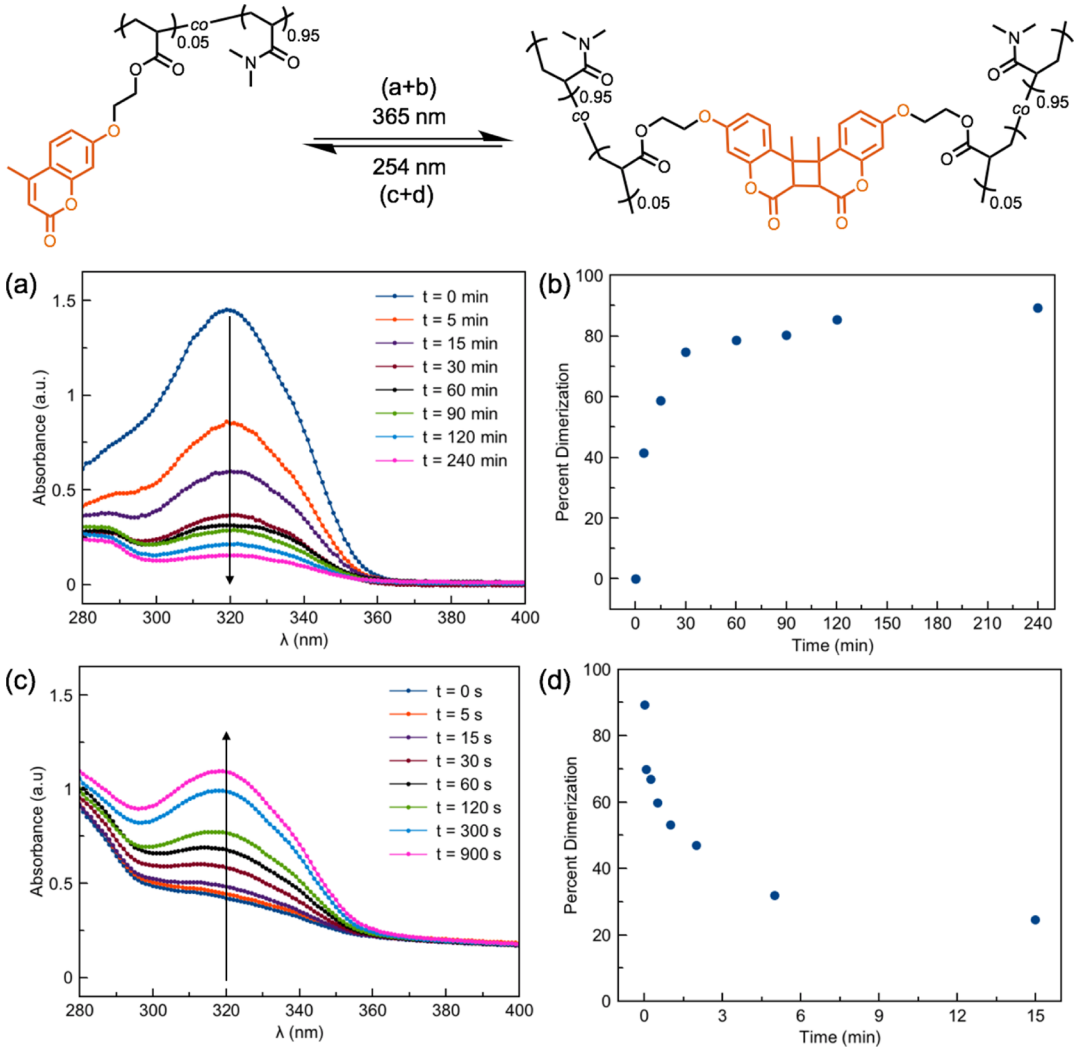

Figure 3. UV−vis study of dimerization and de-dimerization of P(DMA$_{0.95}$-*co*-CoumAc$_{0.05}$). (a) As a solution of the DMA/CoumAc copolymer (0.05 wt % in water) was irradiated with long-wave UV (λ_{max} = 365 nm), a decrease in absorbance was observed, corresponding to dimerization of coumarin. (b) Percent coumarin dimerization as a function of the irradiation time at 365 nm. (c) After 4 h irradiation at 365 nm, the solution was irradiated with short-wave UV (λ_{max} = 254 nm), and an increase in absorbance was observed as the coumarin dimers were cleaved. (d) Percent coumarin de-dimerization as a function of the irradiation time at 254 nm.

DOI: 10.1021/acsami.8b02441
ACS Appl. Mater. Interfaces 2018, 10, 16793−16801

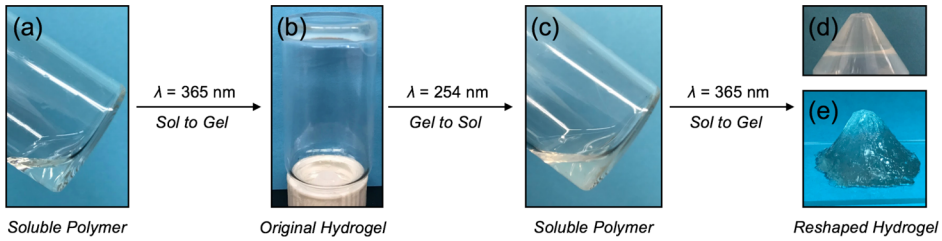

Figure 4. Recycling of coumarin-cross-linked hydrogels using reversible photodimerization. (a) Solution of P($DMA_{0.95}$-*co*-$CoumAc_{0.05}$) in water (5 wt %). (b) Hydrogel formed in a cylindrical vial after irradiation of 5 wt % polymer solution with 365 nm light for 30 min. (c) Resultant polymer solution after irradiating the preformed cylindrical hydrogel with 254 nm light for 30 min. (d) Recycled hydrogel was formed in a conical mold from resolubilized P($DMA_{0.95}$-*co*-$CoumAc_{0.05}$) by irradiating at 365 nm for 30 min. (e) Image of cone-shaped hydrogel after removal from the conical mold.

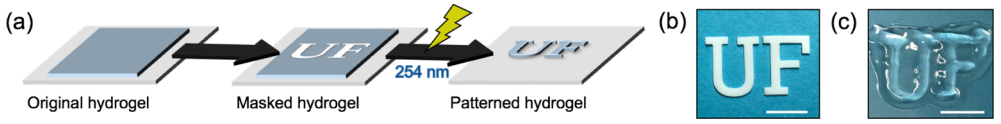

Figure 5. Mask-based photopatterning of coumarin hydrogels. (a) Schematic for post-gelation patterning of coumarin-cross-linked hydrogels. A hydrogel is cast on a glass slide and a Teflon photomask is applied. After irradiation of the gel with short-wave UV light, the exposed areas are etched away, leaving only the desired pattern. (b) Representative Teflon photomask used for photopatterning. (c) Image of a coumarin-cross-linked hydrogel after photopatterning using a photomask. Scale bars are 1 cm.

0.01 wt % under 365 nm light was monitored. Similar reaction kinetics were observed regardless of the polymer concentration, with the extent of dimerization reaching between 70 and 80% for each sample (Figure S19). Furthermore, dimerization kinetics of P($DMA_{0.99}$-*co*-$CoumAc_{0.01}$) were studied at comparable coumarin concentrations to the 5 mol % copolymer (i.e., polymer concentrations of 0.05, 0.10, and 0.25 wt %). Within this series, similar results were again obtained in which comparable extents of dimerization were measured after 4 h of irradiation (Figure S20). When comparing the dimerization processes, it was discovered that the rate of dimerization increased with increasing coumarin content in the copolymer (Figure S21).

On the basis of these results, the polymer concentration was increased further to study the gelation behavior. Solutions of all prepolymers were screened at concentrations varying from 5 to 30 wt %. Although all polymers tested are moderately water-soluble, those with 1 mol % coumarin are significantly more so, as evidenced by their faster dissolution times and greater solution clarity. As expected, irradiation with long-wave UV led to rapid coumarin dimerization, resulting in gelation of the prepolymers in less than 30 min. Compared to most other methods of photo-cross-linking, no external initiator was necessary, potentially allowing for curing in the presence of cells or other radical-sensitive compounds. Oscillatory shear rheology was used to measure the moduli of coumarin-cross-linked hydrogels (Figures S22–S25 and Table S1). Storage moduli were obtained in the range of 10^2–10^3 Pa, values that are on the order of soft tissues such as brain, lymph nodes, and liver tissues.[66] Control over the mechanical properties of hydrogels is vital, as the stiffness of the support medium has been shown to directly impact cell differentiation and morphology.[67] Therefore, to investigate the suitability of coumarin-cross-linked hydrogels for biomedical applications, the viability of human mammary epithelial (MCF-10A) cells exposed to coumarin-containing polymers and hydrogels under various conditions was studied (Figure S26). First, a precured 10 wt % P($DMA_{0.95}$-*co*-$CoumAc_{0.05}$) hydrogel was placed in cell-growth media with plated cells, resulting in only a small decrease in cell viability. Next, cells were prepared with coumarin copolymer solution (i.e., cells plated with solution added on top or cells dispersed within the coumarin solution) and subsequently exposed to UV light to induce gelation. In all cases when UV light was applied, a sharp decrease in the cell viability was observed. Interestingly, suspending the cells in an aqueous solution of the coumarin copolymer increased the cell survival relative to control measurements, possibly because of the attenuation of the applied light through absorption and subsequent photodimerization. These results indicate that the poly(DMA) (PDMA)/coumarin copolymers (and their resultant hydrogels) are not acutely toxic, but a more mild gelation stimulus is necessary to cure the hydrogel with cells present.

The retro-dimerization reaction was examined further for its utility in gel reversal. An aqueous solution (5 wt % polymer, Figure 4a) of P($DMA_{0.95}$-*co*-$CoumAc_{0.05}$) in a cylindrical vial was cured with long-wave UV light for 30 min to form a covalent hydrogel (Figure 4b). This hydrogel was then irradiated with a 254 nm lamp. After 30 min, it was apparent that the gel exposed to UV-C irradiation reverted to an uncross-linked form, as evidenced by its re-solubilization in water (Figure 4c). GPC analysis of the degraded hydrogels suggested a low degree of branching after degradation, as would be expected because of the equilibrium that is established during retrocyclization (Figures S27 and S2). These results suggested that these hydrogels could be readily remolded into different shapes through iterative solubilization-gelation cycles. To examine this possibility, the polymer solution after initial degradation was transferred to a conical mold and re-cured under 365 nm light to generate a reshaped hydrogel (Figure 4d,e). To further examine the efficiency of multiple cycles of dimerization and retrocyclization, UV–vis spectroscopy was used to monitor the processes in solution [0.05 wt % P($DMA_{0.95}$-*co*-$CoumAc_{0.05}$)]. As shown in Figure S29, a majority of coumarin dimers were reverted back to their monomeric form after two dimerization and retrocyclization cycles.

After these initial results, the materials were examined for use in photopatterned gels (Figure 5a). A hydrogel was formed on a glass slide by irradiating a 5 wt % solution of P($DMA_{0.95}$-*co*-$CoumAc_{0.05}$) with long-wave UV light. The slide was then immersed in water to equilibrate the water content of the hydrogel and avoid additional swelling after photoetching. Next, a photomask was placed on top of the hydrogel (Figure 5b), and

DOI: 10.1021/acsami.8b02441
ACS Appl. Mater. Interfaces 2018, 10, 16793–16801

the material was irradiated with short-wave UV to degrade exposed regions of the gel. After rinsing away the de-cross-linked polymer by soaking in water, a hydrogel in the shape of the photomask remained (Figure 5c). This methodology was extended to photomasks with various patterns (Figure S30).

Traditional mask-based photoetching as described above suffers from the need to etch uniformly in one direction, which severely limits the ability to create a controlled structure in the third dimension, perpendicular to the photomask. To improve upon these limitations in etching depth by many orders of magnitude, 3D printing can be employed to fabricate more complex structures, such as tubular or spherical objects with hollow interiors.[68,69] A recent advancement in soft-matter additive manufacturing has provided an avenue for the writing of polymeric hydrogels directly into a granular microgel medium.[49] By eliminating the effects of surface tension and gravity, precise objects with high aspect ratios and high levels of detail may be produced with this technique. We reasoned that sacrificial coumarin-cross-linked hydrogels could assist in removing packed microgels from within cylindrical shells while avoiding significant agitation or damage to the permanent hydrogel structure. Hollow objects could therefore be created by printing and curing the degradable coumarin-based copolymer core inside a nondegradable polymer shell. Inducing the reverse reaction of the coumarin dimer would then liquefy the core and leave behind a cross-linked hydrogel shell.

A tube consisting of nelfilcon A [cross-linkable poly(vinyl alcohol), PVA] as the permanent exterior and P($DMA_{0.95}$-*co*-$CoumAc_{0.05}$) as the sacrificial interior was printed into a jammed microgel support medium (Figure 6a and Supporting Information Movie S1). To examine the quality of printing two unique prepolymers into a single material, confocal microscopy was performed on a cross section of the printed tube. In this process, green fluorescent beads were mixed with the PVA prepolymer and red fluorescent beads were mixed with the coumarin prepolymer before printing and curing. In Figure 6b, it is clear that there is an outer green ring (PVA) surrounding the inner red cylinder (coumarin copolymer). Importantly, no mixing of the red and green layers is observed, suggesting the presence of two discretely cross-linked gels in close proximity to one another. Furthermore, a solid cylinder was obtained following cross-linking of both layers with long-wave UV irradiation (Figure 6c). A cross-sectional image of a solid cylinder (Figure 6d) reveals the presence of both intact gels, the PVA gel wall and the coumarin gel interior, which were stained with Reactive Blue 4 dye for contrast. This printed object was then irradiated with short-wave UV for 3 h and soaked in a water bath overnight to remove any remaining soluble coumarin polymers. The resulting hollow PVA tube collapsed under its own weight when removed from water, indicating complete removal of the interior gel (Figure 6e). After coumarin gel reversal, the remaining tube was dyed with Reactive Blue 4. Imaging the cross section of the object clearly showed the remaining PVA ring and that the coumarin gel was no longer present (Figure 6f). Indeed, the resulting hollow hydrogel tube was able to sustain the flow of water (Figure 6g and Supporting Information Movie S2).

The printing process was extended to access another complex architecture—a hollow hydrogel sphere—that is not readily prepared by conventional hydrogel molding procedures (Supporting Information Movie S3). Again, nelfilcon A was employed as the permanently cross-linked shell, with a 30 wt % solution of P($DMA_{0.99}$-*co*-$CoumAc_{0.01}$) as the sacrificial core

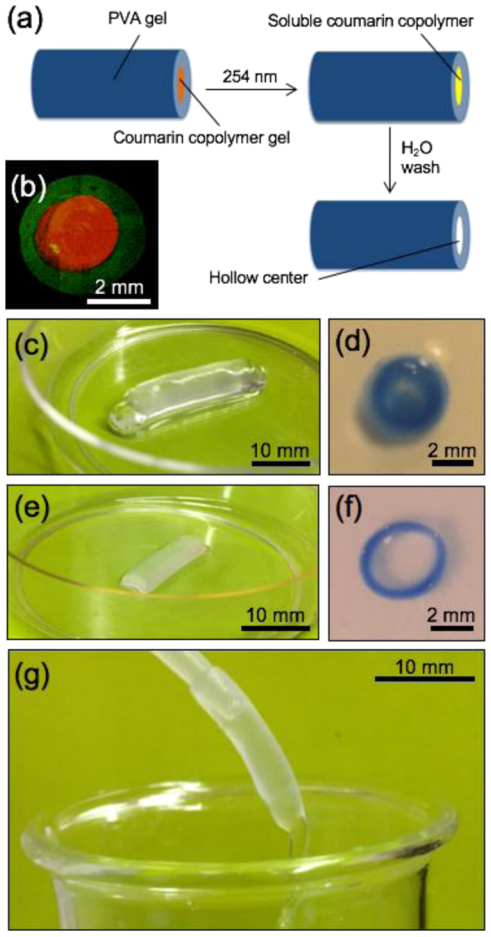

Figure 6. Formation of a 3D-printed hollow hydrogel tube. (a) Solution of the coumarin copolymer was printed into a cylinder, and the PVA solution was printed around the exterior to generate a bilayered cylinder. Following cross-linking, a solid cylinder with a coumarin network in the interior and an outer PVA layer was obtained. Photoinduced de-cross-linking and removal of the interior gel left a hollow hydrogel structure. (b) Green fluorescent beads were mixed with the PVA prepolymer, and red fluorescent beads were mixed with the coumarin prepolymer. Confocal microscopy of a cross-sectional area of the cross-linked tube indicated the quality of the print, displaying a green ring surrounding the red interior with a lack of mixing of the two polymers. (c) Photograph of PVA tube filled with a cross-linked coumarin hydrogel. (d) Photograph of the cylinder cross section directly immediately after printing and cross-linking showed a solid material throughout the entire diameter (stained with Reactive Blue 4 dye for contrast). (e) Following irradiation with short-wave UV light and removal of the resulting soluble coumarin copolymers, a hollow PVA tube remained. (f) After reverting the coumarin gel to soluble polymers and rinsing with water, the cross-sectional image indicated a complete removal of the interior coumarin gel while the intact PVA shell remained (stained with Reactive Blue 4 dye for contrast). (g) Hollow PVA tube was capable of sustaining liquid flow through its cavity.

(Figure 7a). After printing and curing these materials, a solid spherical hydrogel was obtained (Figure 7b). Upon cutting the sphere in half, a solid hemisphere was obtained (Figure 7c), and a dye solution could be suspended on top of the solid coumarin hydrogel interior (Figure 7d). An intact sphere was submerged in water and exposed to short-wave UV irradiation, at which time the interior coumarin hydrogel was solubilized. The result of this process was de-crosslinking of the core of the material, yielding a hollow hydrogel sphere after passive diffusion of the soluble

DOI: 10.1021/acsami.8b02441
ACS Appl. Mater. Interfaces 2018, 10, 16793−16801

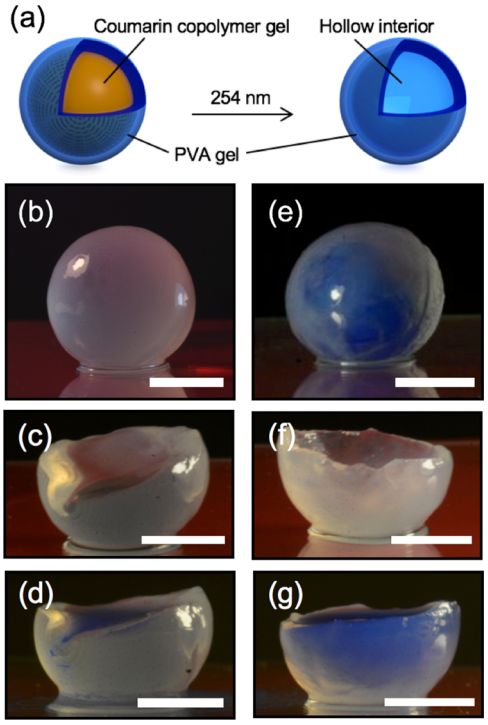

Figure 7. Formation of a 3D-printed hollow hydrogel sphere. (a) Core of the hydrogel sphere is composed of the PDMA/coumarin copolymer and the shell of nelfilcon A. Following cross-linking, a solid sphere with a coumarin network in the interior and an outer PVA layer was obtained. Reversal and removal of the interior gel left a hollow hydrogel structure. (b) Photograph of the PVA sphere filled with a cross-linked coumarin hydrogel. (c) Photograph of solid hydrogel sphere cut in half. (d) Oil-based dye solution was suspended on top of the solid coumarin interior, displaying the in-tact core−shell hydrogel. (e) Photograph of a hollow hydrogel sphere after degradation of the coumarin gel. The interior was filled with a blue oil-based dye solution to provide contrast. (f) Photograph of a hollow hydrogel sphere cut in half. (g) Hemisphere was filled with a blue oil-based dye solution to provide contrast. All scale bars are 5 mm.

polymer from the interior of the object. To confirm that the interior of the sphere was hollow, a blue oil-based dye solution was injected into the sphere, which suggested the absence of a hydrogel core (Figure 7e). Furthermore, upon cutting the sphere in half, the resultant "bowl-shaped" hemisphere was filled with a dye solution, reinforcing that the coumarin hydrogel had been successfully removed from the interior (Figure 7f,g). These results indicate that application of a sacrificial hydrogel to soft-matter additive manufacturing allows for the development of hollow hydrogel constructs that are difficult or impossible to produce by alternative methods.

CONCLUSIONS

In summary, we have developed hydrogels composed of polymers cross-linked by coumarin dimers. Radical copolymerization of coumarin-containing vinyl monomers with a water-soluble comonomer yielded water-soluble copolymers that, upon irradiation with long-wave UV, were cured into free-standing hydrogels. Because these materials were bridged by coumarin-based cyclobutane dimers, they could be reverted back to soluble copolymers upon exposure to short-wave UV light. Importantly, the resolubilized polymers could be cured a second time, providing recyclability of the polymeric hydrogel.

The reversible nature of the cross-links also allowed the hydrogels to be photopatterned. A uniform hydrogel was prepared and masked such that only unmasked areas were exposed to short-wave UV. Therefore, only the exposed regions were de-crosslinked and etched away, leaving a desired pattern imprinted in the hydrogel. Moreover, traditional limitations of mask-based photoablation (e.g., a requirement for uniform etching in one direction) can be circumvented by using a recently developed soft-matter 3D printing technology. In this process, the combination of a nondegradable hydrogel with coumarin-linked hydrogels provided a means to selective etching of a printed material. As an example, we prepared 3D-printed hydrogel structures composed of a nondegradable PVA wall and a degradable P(DMA-*co*-CoumAc) interior. Upon exposure of the entire hydrogel structure to short-wave UV, the interior was reverted to the soluble prepolymer that was readily washed away. However, the PVA gel was unaffected, leaving only the wall behind and cleanly forming hollow hydrogel spheres and cylinders. This methodology can, in principle, be further extended to the formation of branched networks reminiscent of vasculature, or multicompartmental hollow constructs. In addition, the coumarin groups needed for reversible cross-linking could be appended to pre-existing polymers by post-polymerization modification,[70,71] increasing the diversity of accessible polymer compositions and architectures.[72]

The materials in this work display low cytotoxicity, suggesting potential use in the biomedical arena. One current drawback in this respect is the use of UV irradiation for hydrogel curing; although the materials themselves are not harmful to embedded cells, exposure to high-power, long-wave UV irradiation for only 5 min leads to cell death after 24 h. Although the current materials may be useful for applications in which cells are not physically encapsulated within the network, developing a system that cures upon exposure to a more benign stimulus may allow this. Further, integrating a mechanism for degradation of the hydrogel under mild conditions would allow for straightforward cell harvesting and further facilitate the use of these hydrogels as cell scaffolds.

ASSOCIATED CONTENT

Supporting Information

The Supporting Information is available free of charge on the ACS Publications website at DOI: 10.1021/acsami.8b02441.

Materials, instrumentation, and methods; detailed experimental procedures; ^{1}H NMR characterization of intermediates, monomers, and polymers; gel permeation chromatograms of copolymers; UV−vis and FT-IR spectroscopy measurements; dimerization and retrocyclization kinetics for P(DMA$_{1-y}$-*co*-CoumAAm$_y$); concentration-dependent dimerization kinetics and dimerization/cycloreversion cycling; hydrogel rheological measurements; cell viability assay of the MCF-10A cell line; and images of photopatterned hydrogels (PDF)

Printing of a hydrogel tube into a jammed microgel support medium (MPG)

Printing of a hydrogel sphere into a jammed microgel support medium (MPG)

Extension of the printing process to access a complex architecture (MPG)

DOI: 10.1021/acsami.8b02441
ACS Appl. Mater. Interfaces 2018, 10, 16793−16801

AUTHOR INFORMATION

Corresponding Author

*E-mail: sumerlin@chem.ufl.edu.

ORCID

Christopher P. Kabb: 0000-0002-5125-2705

Brent S. Sumerlin: 0000-0001-5749-5444

Author Contributions

The manuscript was written through contributions of all authors.

Funding

This material is based on work supported by the National Science Foundation (DMR-1606410 and DMR-1352043). Acknowledgment is made to the University of Florida Research Opportunity Seed Fund for partial support of this research. C.P.K. gratefully acknowledges fellowship support from Eastman Chemical Company.

Notes

The authors declare no competing financial interest.

REFERENCES

(1) Wojtecki, R. J.; Meador, M. A.; Rowan, S. J. Using the Dynamic Bond to Access Macroscopically Responsive Structurally Dynamic Polymers. *Nat. Mater.* **2011**, *10*, 14−27.

(2) Maddipatla, M. V. S. N.; Wehrung, D.; Tang, C.; Fan, W.; Oyewumi, M. O.; Miyoshi, T.; Joy, A. Photoresponsive Coumarin Polyesters That Exhibit Cross-Linking and Chain Scission Properties. *Macromolecules* **2013**, *46*, 5133−5140.

(3) Nagata, M.; Yamamoto, Y. Photoreversible Poly(Ethylene Glycol)s with Pendent Coumarin Group and Their Hydrogels. *React. Funct. Polym.* **2008**, *68*, 915−921.

(4) Liu, W.-X.; Zhang, C.; Zhang, H.; Zhao, N.; Yu, Z.-X.; Xu, J. Oxime-Based and Catalyst-Free Dynamic Covalent Polyurethanes. *J. Am. Chem. Soc.* **2017**, *139*, 8678.

(5) Chao, A.; Negulescu, I.; Zhang, D. Dynamic Covalent Polymer Networks Based on Degenerative Imine Bond Exchange: Tuning the Malleability and Self-Healing Properties by Solvent. *Macromolecules* **2016**, *49*, 6277−6284.

(6) Mukherjee, S.; Hill, M. R.; Sumerlin, B. S. Self-Healing Hydrogels Containing Reversible Oxime Crosslinks. *Soft Matter* **2015**, *11*, 6152−6161.

(7) Sun, H.; Kabb, C. P.; Dai, Y.; Hill, M. R.; Ghiviriga, I.; Bapat, A. P.; Sumerlin, B. S. Macromolecular Metamorphosis Via Stimulus-Induced Transformations of Polymer Architecture. *Nat. Chem.* **2017**, *9*, 817−823.

(8) Patil, S. S.; Torris, A.; Wadgaonkar, P. P. Healable Network Polymers Bearing Flexible Poly(Lauryl Methacrylate) Chains Via Thermo-Reversible Furan-Maleimide Diels−Alder Reaction. *J. Polym. Sci., Part A: Polym. Chem.* **2017**, *55*, 2700−2712.

(9) Lyon, G. B.; Baranek, A.; Bowman, C. N. Scaffolded Thermally Remendable Hybrid Polymer Networks. *Adv. Funct. Mater.* **2016**, *26*, 1477−1485.

(10) Berg, G. J.; Gong, T.; Fenoli, C. R.; Bowman, C. N. A Dual-Cure, Solid-State Photoresist Combining a Thermoreversible Diels−Alder Network and a Chain Growth Acrylate Network. *Macromolecules* **2014**, *47*, 3473−3482.

(11) Feillée, N.; Chemtob, A.; Ley, C.; Croutxé-Barghorn, C.; Allonas, X.; Ponche, A.; Le Nouen, D.; Majjad, H.; Jacomine, L. Photoinduced Cross-Linking of Dynamic Poly(Disulfide) Films Via Thiol Oxidative Coupling. *Macromol. Rapid Commun.* **2016**, *37*, 155−160.

(12) Yoon, J. A.; Kamada, J.; Koynov, K.; Mohin, J.; Nicolaÿ, R.; Zhang, Y.; Balazs, A. C.; Kowalewski, T.; Matyjaszewski, K. Self-Healing Polymer Films Based on Thiol−Disulfide Exchange Reactions and Self-Healing Kinetics Measured Using Atomic Force Microscopy. *Macromolecules* **2012**, *45*, 142−149.

(13) Vogt, A. P.; Sumerlin, B. S. Temperature and Redox Responsive Hydrogels from ABA Triblock Copolymers Prepared by RAFT Polymerization. *Soft Matter* **2009**, *5*, 2347−2351.

(14) Brooks, W. L. A.; Sumerlin, B. S. Synthesis and Applications of Boronic Acid-Containing Polymers: From Materials to Medicine. *Chem. Rev.* **2016**, *116*, 1375−1397.

(15) Deng, C. C.; Brooks, W. L. A.; Abboud, K. A.; Sumerlin, B. S. Boronic Acid-Based Hydrogels Undergo Self-Healing at Neutral and Acidic pH. *ACS Macro Lett.* **2015**, *4*, 220−224.

(16) Cash, J. J.; Kubo, T.; Bapat, A. P.; Sumerlin, B. S. Room-Temperature Self-Healing Polymers Based on Dynamic-Covalent Boronic Esters. *Macromolecules* **2015**, *48*, 2098−2106.

(17) Cromwell, O. R.; Chung, J.; Guan, Z. Malleable and Self-Healing Covalent Polymer Networks through Tunable Dynamic Boronic Ester Bonds. *J. Am. Chem. Soc.* **2015**, *137*, 6492−6495.

(18) Blasco, E.; Sims, M. B.; Goldmann, A. S.; Sumerlin, B. S.; Barner-Kowollik, C. 50th Anniversary Perspective: Polymer Functionalization. *Macromolecules* **2017**, *50*, 5215−5252.

(19) Tomlinson, W. J.; Chandross, E. A.; Fork, R. L.; Pryde, C. A.; Lamola, A. A. Reversible Photodimerization: A New Type of Photochromism. *Appl. Opt.* **1972**, *11*, 533−548.

(20) Azagarsamy, M. A.; McKinnon, D. D.; Alge, D. L.; Anseth, K. S. Coumarin-Based Photodegradable Hydrogel: Design, Synthesis, Gelation, and Degradation Kinetics. *ACS Macro Lett.* **2014**, *3*, 515−519.

(21) Gnanaguru, K.; Ramasubbu, N.; Venkatesan, K.; Ramamurthy, V. A Study on the Photochemical Dimerization of Coumarins in the Solid State. *J. Org. Chem.* **1985**, *50*, 2337−2346.

(22) Chujo, Y.; Sada, K.; Saegusa, T. Polyoxazoline Having a Coumarin Moiety as a Pendant Group. Synthesis and Photogelation. *Macromolecules* **1990**, *23*, 2693−2697.

(23) Becker, H. D. Unimolecular Photochemistry of Anthracenes. *Chem. Rev.* **1993**, *93*, 145−172.

(24) Setlow, R. B. Cyclobutane-Type Pyrimidine Dimers in Polynucleotides. *Science* **1966**, *153*, 379−386.

(25) Mochizuki, E.; Tohnai, N.; Wang, Y.; Saito, T.; Inaki, Y.; Miyata, M.; Yasui, N.; Kai, Y. Reversible Photodimerization of Ester Derivatives of Thymine Having Long Alkyl Chains in Solid Film. *Polym. J.* **2000**, *32*, 492−500.

(26) López-Vilanova, L.; Martinez, I.; Corrales, T.; Catalina, F. Photoreversible Crosslinking of Poly-(Ethylene-Butyl-Acrylate) Copolymers Functionalized with Coumarin Chromophores Using Microwave Methodology. *React. Funct. Polym.* **2014**, *85*, 28−35.

(27) Mal, N. K.; Fujiwara, M.; Tanaka, Y. Photocontrolled Reversible Release of Guest Molecules from Coumarin-Modified Mesoporous Silica. *Nature* **2003**, *421*, 350−353.

(28) Chen, Y.; Wang, Z.; He, Y.; Yoon, Y. J.; Jung, J.; Zhang, G.; Lin, Z. Light-Enabled Reversible Self-Assembly and Tunable Optical Properties of Stable Hairy Nanoparticles. *Proc. Natl. Acad. Sci. U.S.A.* **2018**, *115*, No. E1391.

(29) Trenor, S. R.; Shultz, A. R.; Love, B. J.; Long, T. E. Coumarins in Polymers: From Light Harvesting to Photo-Cross-Linkable Tissue Scaffolds. *Chem. Rev.* **2004**, *104*, 3059−3078.

(30) Govindarajan, S. R.; Xu, Y.; Swanson, J. P.; Jain, T.; Lu, Y.; Choi, J.-W.; Joy, A. A Solvent and Initiator Free, Low-Modulus, Degradable Polyester Platform with Modular Functionality for Ambient-Temperature 3D Printing. *Macromolecules* **2016**, *49*, 2429−2437.

(31) Matsuda, T.; Mizutani, M.; Arnold, S. C. Molecular Design of Photocurable Liquid Biodegradable Copolymers. 1. Synthesis and Photocuring Characteristics. *Macromolecules* **2000**, *33*, 795−800.

(32) Matsuda, T.; Mizutani, M. Molecular Design of Photocurable Liquid Biodegradable Copolymers. 2. Synthesis of Coumarin-Derivatized Oligo(Methacrylate)s and Photocuring. *Macromolecules* **2000**, *33*, 791−794.

(33) Tamate, R.; Ueki, T.; Kitazawa, Y.; Kuzunuki, M.; Watanabe, M.; Akimoto, A. M.; Yoshida, R. Photo-Dimerization Induced Dynamic Viscoelastic Changes in ABA Triblock Copolymer-Based Hydrogels for 3D Cell Culture. *Chem. Mater.* **2016**, *28*, 6401−6408.

(34) Jiang, M.; Paul, N.; Bieniek, N.; Buckup, T.; Hampp, N.; Motzkus, M. Photocleavage of Coumarin Dimers Studied by Femtosecond UV Transient Absorption Spectroscopy. *Phys. Chem. Chem. Phys.* **2017**, *19*, 4597−4606.

DOI: 10.1021/acsami.8b02441
ACS Appl. Mater. Interfaces 2018, 10, 16793−16801

(35) Ling, J.; Rong, M. Z.; Zhang, M. Q. Coumarin Imparts Repeated Photochemical Remendability to Polyurethane. *J. Mater. Chem.* **2011**, *21*, 18373−18380.
(36) Caliari, S. R.; Burdick, J. A. A Practical Guide to Hydrogels for Cell Culture. *Nat. Meth.* **2016**, *13*, 405−414.
(37) Khetan, S.; Burdick, J. A. Patterning Hydrogels in Three Dimensions Towards Controlling Cellular Interactions. *Soft Matter* **2011**, *7*, 830−838.
(38) Ouyang, L.; Highley, C. B.; Sun, W.; Burdick, J. A. A Generalizable Strategy for the 3D Bioprinting of Hydrogels from Nonviscous Photo-Crosslinkable Inks. *Adv. Mater.* **2017**, *29*, 1604983.
(39) Zhang, M.; Vora, A.; Han, W.; Wojtecki, R. J.; Maune, H.; Le, A. B. A.; Thompson, L. E.; McClelland, G. M.; Ribet, F.; Engler, A. C.; Nelson, A. Dual-Responsive Hydrogels for Direct-Write 3D Printing. *Macromolecules* **2015**, *48*, 6482−6488.
(40) Ito, H.; Willson, C. G.; Frechet, J. M. J. New UV Resists with Negative or Positive Tone. *Digest of Technical Papers—Symposium on VLSI Technology*, 1982; pp 86−87.
(41) DeForest, C. A.; Polizzotti, B. D.; Anseth, K. S. Sequential Click Reactions for Synthesizing and Patterning Three-Dimensional Cell Microenvironments. *Nat. Mater.* **2009**, *8*, 659−664.
(42) Peng, H.; Wang, C.; Xi, W.; Kowalski, B. A.; Gong, T.; Xie, X.; Wang, W.; Nair, D. P.; McLeod, R. R.; Bowman, C. N. Facile Image Patterning Via Sequential Thiol−Michael/Thiol−Yne Click Reactions. *Chem. Mater.* **2014**, *26*, 6819−6826.
(43) Xi, W.; Peng, H.; Aguirre-Soto, A.; Kloxin, C. J.; Stansbury, J. W.; Bowman, C. N. Spatial and Temporal Control of Thiol-Michael Addition Via Photocaged Superbase in Photopatterning and Two-Stage Polymer Networks Formation. *Macromolecules* **2014**, *47*, 6159−6165.
(44) Gordon, M. B.; French, J. M.; Wagner, N. J.; Kloxin, C. J. Dynamic Bonds in Covalently Crosslinked Polymer Networks for Photoactivated Strengthening and Healing. *Adv. Mater.* **2015**, *27*, 8007−8010.
(45) Kloxin, A. M.; Kasko, A. M.; Salinas, C. N.; Anseth, K. S. Photodegradable Hydrogels for Dynamic Tuning of Physical and Chemical Properties. *Science* **2009**, *324*, 59−63.
(46) Kloxin, A. M.; Tibbitt, M. W.; Kasko, A. M.; Fairbairn, J. A.; Anseth, K. S. Tunable Hydrogels for External Manipulation of Cellular Microenvironments through Controlled Photodegradation. *Adv. Mater.* **2010**, *22*, 61−66.
(47) Truby, R. L.; Lewis, J. A. Printing Soft Matter in Three Dimensions. *Nature* **2016**, *540*, 371−378.
(48) O'Bryan, C. S.; Bhattacharjee, T.; Niemi, S. R.; Balachandar, S.; Baldwin, N.; Ellison, S. T.; Taylor, C. R.; Sawyer, W. G.; Angelini, T. E. Three-Dimensional Printing with Sacrificial Materials for Soft Matter Manufacturing. *MRS Bull.* **2017**, *42*, 571−577.
(49) Bhattacharjee, T.; Zehnder, S. M.; Rowe, K. G.; Jain, S.; Nixon, R. M.; Sawyer, W. G.; Angelini, T. E. Writing in the Granular Gel Medium. *Sci. Adv.* **2015**, *1*, No. e1500655.
(50) Hinton, T. J.; Jallerat, Q.; Palchesko, R. N.; Park, J. H.; Grodzicki, M. S.; Shue, H.-J.; Ramadan, M. H.; Hudson, A. R.; Feinberg, A. W. Three-Dimensional Printing of Complex Biological Structures by Freeform Reversible Embedding of Suspended Hydrogels. *Sci. Adv.* **2015**, *1*, No. e1500758.
(51) O'Bryan, C. S.; Bhattacharjee, T.; Hart, S.; Kabb, C. P.; Schulze, K. D.; Chilakala, I.; Sumerlin, B. S.; Sawyer, W. G.; Angelini, T. E. Self-Assembled Micro-Organogels for 3D Printing Silicone Structures. *Sci. Adv.* **2017**, *3*, No. e1602800.
(52) Hinton, T. J.; Hudson, A.; Pusch, K.; Lee, A.; Feinberg, A. W. 3D Printing PDMS Elastomer in a Hydrophilic Support Bath Via Freeform Reversible Embedding. *ACS Biomater. Sci. Eng.* **2016**, *2*, 1781−1786.
(53) Bhattacharjee, T.; Gil, C. J.; Marshall, S. L.; Urueña, J. M.; O'Bryan, C. S.; Carstens, M.; Keselowsky, B.; Palmer, G. D.; Ghivizzani, S.; Gibbs, C. P.; Sawyer, W. G.; Angelini, T. E. Liquid-Like Solids Support Cells in 3D. *ACS Biomater. Sci. Eng.* **2016**, *2*, 1787−1795.
(54) Kolesky, D. B.; Truby, R. L.; Gladman, A. S.; Busbee, T. A.; Homan, K. A.; Lewis, J. A. 3D Bioprinting of Vascularized, Heterogeneous Cell-Laden Tissue Constructs. *Adv. Mater.* **2014**, *26*, 3124−3130.
(55) Highley, C. B.; Rodell, C. B.; Burdick, J. A. Direct 3D Printing of Shear-Thinning Hydrogels into Self-Healing Hydrogels. *Adv. Mater.* **2015**, *27*, 5075−5079.
(56) Wolff, T.; Görner, H. Photodimerization of Coumarin Revisited: Effects of Solvent Polarity on the Triplet Reactivity and Product Pattern. *Phys. Chem. Chem. Phys.* **2004**, *6*, 368−376.
(57) Chamsaz, E. A.; Sun, S.; Maddipatla, M. V. S. N.; Joy, A. Photoresponsive Polyesters by Incorporation of Alkoxyphenacyl or Coumarin Chromophores Along the Backbone. *Photochem. Photobiol. Sci.* **2014**, *13*, 412−421.
(58) Onbulak, S.; Rzayev, J. Cylindrical Nanocapsules from Photo-Cross-Linkable Core-Shell Bottlebrush Copolymers. *Polym. Chem.* **2015**, *6*, 764−771.
(59) Jiang, J.; Qi, B.; Lepage, M.; Zhao, Y. Polymer Micelles Stabilization on Demand through Reversible Photo-Cross-Linking. *Macromolecules* **2007**, *40*, 790−792.
(60) Amir, R. J.; Albertazzi, L.; Willis, J.; Khan, A.; Kang, T.; Hawker, C. J. Multifunctional Trackable Dendritic Scaffolds and Delivery Agents. *Angew. Chem., Int. Ed.* **2011**, *50*, 3425−3429.
(61) Dübner, M.; Gevrek, T. N.; Sanyal, A.; Spencer, N. D.; Padeste, C. Fabrication of Thiol−Ene "Clickable" Copolymer-Brush Nanostructures on Polymeric Substrates Via Extreme Ultraviolet Interference Lithography. *ACS Appl. Mater. Interfaces* **2015**, *7*, 11337−11345.
(62) Shaughnessy, K. H.; Kim, P.; Hartwig, J. F. A Fluorescence-Based Assay for High-Throughput Screening of Coupling Reactions. Application to Heck Chemistry. *J. Am. Chem. Soc.* **1999**, *121*, 2123−2132.
(63) Chen, Y.; Wu, J.-D. Preparation and Photoreaction of Copolymers Derived from N-(1-Phenylethyl)Acrylamide and 7-Acryloyloxy-4-Methyl Coumarin. *J. Polym. Sci., Part A: Polym. Chem.* **1994**, *32*, 1867−1875.
(64) Chen, Y.; Geh, J.-L. Copolymers Derived from 7-Acryloyloxy-4-Methylcoumarin and Acrylates: 2. Reversible Photocrosslinking and Photocleavage. *Polymer* **1996**, *37*, 4481−4486.
(65) Trenor, S. R.; Long, T. E.; Love, B. J. Photoreversible Chain Extension of Poly(Ethylene Glycol). *Macromol. Chem. Phys.* **2004**, *205*, 715−723.
(66) Levental, I.; Georges, P. C.; Janmey, P. A. Soft Biological Materials and Their Impact on Cell Function. *Soft Matter* **2007**, *3*, 299−306.
(67) Butcher, D. T.; Alliston, T.; Weaver, V. M. A Tense Situation: Forcing Tumour Progression. *Nat. Rev. Cancer* **2009**, *9*, 108−122.
(68) Paulsen, S. J.; Miller, J. S. Tissue Vascularization through 3D Printing: Will Technology Bring Us Flow? *Dev. Dyn.* **2015**, *244*, 629−640.
(69) Lee, V. K.; Kim, D. Y.; Ngo, H.; Lee, Y.; Seo, L.; Yoo, S.-S.; Vincent, P. A.; Dai, G. Creating Perfused Functional Vascular Channels Using 3D Bio-Printing Technology. *Biomaterials* **2014**, *35*, 8092−8102.
(70) Easterling, C. P.; Kubo, T.; Orr, Z. M.; Fanucci, G. E.; Sumerlin, B. S. Synthetic Upcycling of Polyacrylates through Organocatalyzed Post-Polymerization Modification. *Chem. Sci.* **2017**, *8*, 7705−7709.
(71) Kubo, T.; Bentz, K. C.; Powell, K. C.; Figg, C. A.; Swartz, J. L.; Tansky, M.; Chauhan, A.; Savin, D. A.; Sumerlin, B. S. Modular and Rapid Access to Amphiphilic Homopolymers Via Successive Chemoselective Post-Polymerization Modification. *Polym. Chem.* **2017**, *8*, 6028−6032.
(72) Bachler, P. R.; Forry, K. E.; Sparks, C. A.; Schulz, M. D.; Wagener, K. B.; Sumerlin, B. S. Modular Segmented Hyperbranched Copolymers. *Polym. Chem.* **2016**, *7*, 4155−4159.

DOI: 10.1021/acsami.8b02441
ACS Appl. Mater. Interfaces 2018, 10, 16793−16801

Supplementary Information for

Photoreversible Covalent Hydrogels for Soft-Matter Additive Manufacturing

Christopher P. Kabb,[1] Christopher S. O'Bryan,[2] Christopher C. Deng,[1] Thomas E. Angelini,[2,3,4] Brent S. Sumerlin[1,*]

[1] George & Josephine Butler Polymer Research Laboratory, Center for Macromolecular Science & Engineering, Department of Chemistry, University of Florida, Gainesville, FL 32611, USA.
[2] Department of Mechanical and Aerospace Engineering, University of Florida, Gainesville, FL 32611, USA.
[3] J. Crayton Pruitt Family Department of Biomedical Engineering, University of Florida, Gainesville, FL 32611, USA.
[4] Institute for Cell and Regenerative Medicine, University of Florida, Gainesville, FL 32611, USA.

*Corresponding author: sumerlin@chem.ufl.edu

Supplementary Information:

Table of Contents

Materials

All chemicals were used as received unless otherwise noted. Azobisisobutyronitrile (AIBN, Sigma, 98%) was recrystallized from ethanol and dried *in vacuo* prior to use. *N*,*N*-Dimethylacrylamide (DMA, Aldrich, 99%) was passed through a column of basic alumina to remove inhibitors and acidic impurities prior to polymerization. Di-*tert*-butyl dicarbonate (99%), 4-methylumbelliferone (≥98%), 2-bromoethanol (95%), 2-bromoethylamine hydrobromide (99%), acryloyl chloride (>97%), sodium bicarbonate (>99%), and 1,4-dioxane (>99%) were purchased from Sigma-Aldrich. Trifluoroacetic acid (99%), sodium chloride (ACS), chloroform (ACS), dichloromethane (ACS), sodium sulfate (ACS), *N*,*N*-dimethylformamide (DMF, ACS), acetone (ACS), and ethanol (100%) were purchased from Fisher Scientific. Triethylamine (TEA, 99%) was purchased from Alfa Aesar. Potassium carbonate (ACS) and hydrochloric acid (ACS) were purchased from EMD Millipore. Ashland 980 Carbomer was obtained from Ashland. Nelfilcon A was obtained from Alcon Laboratories, Inc.

Instrumentation and Methods

Nuclear Magnetic Resonance (NMR) Spectroscopy. ^{1}H and ^{13}C NMR spectra were recorded in $CDCl_3$ or DMSO-d_6 using an Inova 500 MHz spectrometer at 25 ˚C.

Electrospray Ionization-High Resolution Mass Spectrometry (ESI-HRMS). HRMS was carried out using an Agilent 6220 TOF-MS mass spectrometer in the electrospray ionization (ESI) mode.

Gel Permeation Chromatography (GPC). Molecular weight and polydispersity were determined by gel permeation chromatography in *N,N*-dimethylacetamide (DMAc) with 50 mM LiCl at 50 °C and a flow rate of 1.0 mL min^{-1} (Agilent isocratic pump, degasser, and autosampler, columns: Viscogel I-series 5 μm guard + two ViscoGel I-series G3078 mixed bed columns: molecular weight range 0−20 × 10^3 and 0−10 × 10^5 g mol^{-1}). Detection consisted of a Wyatt Optilab T-rEX refractive index detector operating at 658 nm and a Wyatt miniDAWN Treos light scattering detector operating at 659 nm. Absolute molecular weights and polydispersities were calculated using the Wyatt ASTRA software and the d*n*/dc for poly(*N*,*N*-dimethylacrylamide) in the GPC eluent (0.0699 mL/g).

UV-Vis Spectroscopy. All measurements were taken using a Molecular Devices SpectraMax M2 Multimode Microplate Reader at 25 °C. Absorbance measurements were conducted with 200 μL of sample on clear 96-well polypropylene microplates (Greiner Bio-One).

Fourier Transform Infrared (FTIR) Spectroscopy. Infrared spectra were collected on a Thermo Nicolet 5700 FT-IR spectrometer equipped with a single bounce diamond stage attenuated total reflectance (ATR) accessory.

UV Irradiation. Long-wave UV irradiation was performed using a commercial UV lamp with an intensity of 7 mW cm^{-2} (measured with General UV513AB Digital UV AB Light Meter calibrated at 365 nm) or in a 400 W, 320 to 390 nm UV flood curing lamp (Sunray). Short-wave UV irradiation was performed in a Stratagene UV Stratalinker 1800 equipped with five 254 nm light bulbs (8 W each).

Cell Viability. MCF-10A (human mammary epithelial cells) were dyed using a Calcien Red-Orange dye prior to passaging. The cells were then passaged, and treated under one of five sets of conditions (pictorial representations in Fig. S26). In (*i*), the cells were plated and viability was measured as a control. In (*ii*), a pre-cured PDMA/coumarin hydrogel was placed into cell growth media on top of plated cells. In (*iii*), the cells were plated and irradiated with 365 nm light for 5 min. In (*iv*), the cells were plated, and a solution of PDMA/coumarin copolymer was introduced. The sample was irradiated with 365 nm light for 5 min to cure the hydrogel. In (*v*), the cells were suspended in a solution of P($DMA_{0.95}$-*co*-$CoumAc_{0.05}$) copolymer (5 wt% in MEGM cell growth media). The solution was dispersed in glass bottom petri dishes (× 4) and subjected to irradiation with 365 nm UV light for 5 min (Sunray flood curing lamp) to cure the hydrogel. After polymerization, additional media was placed on top of the gel with CMFDA (Cell Tracker Green) dye and placed in the incubator for 24 h. After this time, confocal images were taken using the red and green channel. All cells were dyed red by Calcien-Red Orange, while the green cells were those that were dead after the UV curing process.

Oscillatory Shear Rheology. Oscillatory shear rheology was performed on a TA Instruments Discovery Hybrid Rheometer (DHR-2) operating at 25 °C with a 20 mm flat-plate geometry. Frequency sweeps were conducted at 1% strain and strain sweeps were conducted at an angular frequency of 10 rad s^{-1}.

3D Printing. All 3D printing was performed using the methods described by Bhattacharjee *et. al.*[1] Three translational linear stages were equipped with a fourth linear stage as a syringe pump (Newport). Both the syringe pump and translational stages were controlled using custom-written MATLAB scripts and trajectories. Prepolymer solutions were loaded into a glass syringe (Hamilton) with a 26 gauge blunt dispensing needle (McMaster Carr) before being printed into a jammed microgel support material (Ashland 980), prepared at 0.15 wt% and swollen at neutral pH. After printing, polymers were cured using a 400 W, 320 to 390 nm UV flood curing lamp (Sunray) for 10 min. Supplementary Movies 1 and 3 depict example processes for printing two-component hydrogel tubes and spheres, respectively. In these videos, red and/or green insoluble fluorescent beads are added to the polymeric inks to add contrast. The printed materials shown in these videos are not cured and are used solely to demonstrate the procedure for printing complex hydrogel structures.

Procedures

Synthesis of 7-(2-hydroxyethoxy)-4-methylcoumarin

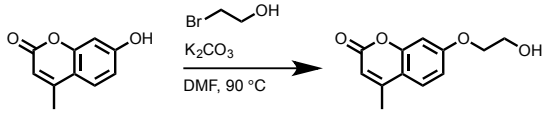

The target compound was synthesized according to previously reported procedures.[2-4] 4-Methylumbelliferone (4.00 g, 22.7 mmol, 1 equiv.) and potassium carbonate (6.23 g, 45.4 mmol, 2 equiv.) were mixed in anhydrous DMF (40 mL) under argon atmosphere. 2-Bromoethanol (2.42 mL, 34.0 mmol, 1.5 equiv.) was added, and the reaction was heated at 90 °C for 18 h. The reaction mixture was cooled to room temperature and poured into ice-cold water. The white precipitate was collected by vacuum filtration and dried *in vacuo*. Yield: 4.7 g (94.0%). ^{1}H NMR (500 MHz, DMSO-d_6): δ (ppm) 7.67-7.63 (d, 1H), 6.97-6.93 (m, 2H), 6.18 (s, 1H), 4.95 (t, 1H), 4.09 (t, 2H), 3.74 (t, 2H), 2.38 (s, 3H).

Synthesis of 7-(2-acryloyloxyethoxy)-4-methylcoumarin (CoumAc)

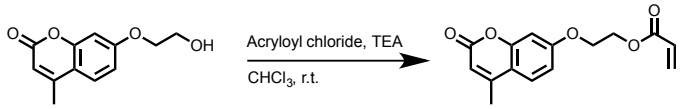

CoumAc was synthesized according to a modified procedure.[2,5] 7-(2-Hydroxyethoxy)-4-methylcoumarin (4.00 g, 18.2 mmol, 1 equiv.) was suspended in chloroform (75 mL) and triethylamine (5.06 mL, 36.3 mmol, 2 equiv.) was added. Acryloyl chloride (2.94 mL, 36.3 mmol, 2 equiv.) was added portionwise under argon and the reaction was stirred at room temperature. After 1 h, additional triethylamine (2.53 mL, 18.2 mmol, 1 equiv.) and acryloyl chloride (1.47 mL, 18.2 mmol, 1 equiv.) were added and the solution was stirred overnight. The reaction mixture was diluted with dichloromethane, washed with brine (100 mL × 2), dried over sodium sulfate, filtered, and concentrated *in vacuo*. The crude product was recrystallized twice from ethanol to yield **CoumAc** as a white powder. Yield: 1.90 g (38.1%). ^{1}H NMR (500 MHz, $CDCl_3$): δ (ppm) 7.51 (d, 1H), 6.89 (dd, 1H), 6.82 (d, 1H), 6.48-6.44 (dd, 1H), 6.20-6.14 (m, 2H), 5.89-5.86 (dd, 1H), 4.55 (t, 2H), 4.28 (t, 2H), 2.39 (s, 3H).

Synthesis of *tert*-butyl 2-bromoethylcarbamate

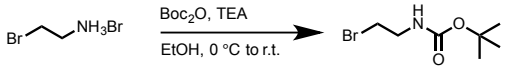

Tert-butyl 2-bromoethylcarbamate was synthesized according to a previous report.[6] 2-Bromoethylamine hydrobromide (5.00 g, 24.4 mmol, 1 equiv.) and triethylamine (5.10 mL, 36.6 mmol, 1.5 equiv.) were dissolved in ethanol (40 mL) and cooled to 0 °C. Di-*tert*-butyl dicarbonate (6.30 g, 29.2 mmol, 1.2 equiv.) was dissolved in ethanol (20 mL) and added dropwise to the slurry. The reaction mixture was warmed to room temperature and stirred for 20 h, concentrated *in vacuo*, and redissolved in H_2O (30 mL). The solution was extracted with ethyl acetate (100 mL × 2), dried over sodium sulfate, filtered and concentrated *in vacuo*. The product was obtained as a colorless oil. Yield: 5.43 g (99.5%). ^{1}H NMR (500 MHz, $CDCl_3$): δ (ppm) 4.94 (br, 1H), 3.53 (t, 2H), 3.45 (t, 2H), 1.45 (s, 9H). ^{13}C NMR (125 MHz, $CDCl_3$): δ (ppm) 146.88, 85.32, 42.49, 32.99, 28.49.

Synthesis of 7-(2-*boc*-aminoethoxy)-4-methylcoumarin

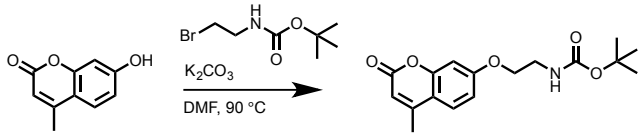

4-Methylumbelliferone (2.93 g, 16.7 mmol, 1 equiv.) and potassium carbonate (4.60 g, 33.3 mmol, 2 equiv.) were stirred in anhydrous DMF (35 mL) under argon. *Tert*-butyl 2-bromoethylcarbamate (5.60 g, 25.0 mmol, 1.5 equiv.) was added portionwise under argon and the reaction mixture was heated to 90 °C. After 18 h, the mixture was cooled to room temperature and precipitated into ice-cold water. The sticky residue was taken up in acetone and dried *in vacuo* to yield the product as a yellow-orange solid. Yield: 1.90 g (35.6%). ^{1}H NMR (500 MHz, DMSO-d_6): δ (ppm) 7.70-7.67 (d, 1H), 7.06-6.93 (m, 3H), 6.21 (s, 1H), 4.01 (t, 2H), 3.32 (t, 2H), 2.39 (s, 3H), 1.38 (s, 9H).

Synthesis of 7-(2-(ammonium trifluoroacetate)ethoxy)-4-methylcoumarin

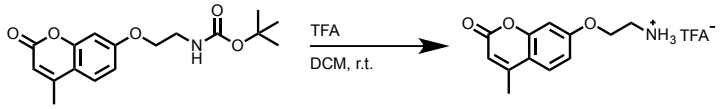

7-(2-*Boc*-aminoethoxy)-4-methylcoumarin (1.90 g, 5.90 mmol, 1 equiv.) was dissolved in anhydrous dichloromethane (50 mL). Trifluoroacetic acid (8.15 mL, 106 mmol, 20 equiv.) was added and the reaction mixture was stirred for 18 h. The orange solution was concentrated *in vacuo* to yield the product as a light brown powder. Yield: 1.99 g (100%). ^{1}H NMR (500 MHz, DMSO-d_6): δ (ppm) 8.10 (br, 3H), 7.71 (d, 1H), 7.03-6.97 (m, 2H), 6.22 (s, 1H), 4.27 (t, 2H), 3.25 (t, 2H), 2.39 (s, 3H).

Synthesis of 7-(2-acrylamidoethoxy)-4-methylcoumarin (CoumAAm)

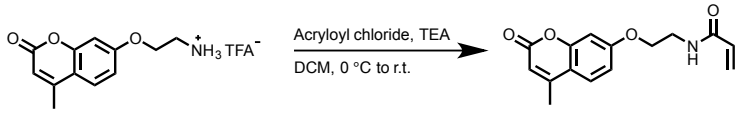

7-(2-(Ammonium trifluoroacetate)ethoxy)-4-methylcoumarin (1.99 g, 6.08 mmol, 1 equiv.) and triethylamine (2.54 mL, 18.2 mmol, 3 equiv.) were dissolved in anhydrous dichloromethane (25 mL) and cooled to 0 °C under argon. Acryloyl chloride (0.98 mL, 12.1 mmol, 2 equiv.) was added dropwise and the reaction mixture was warmed to room temperature. After 18 h, the solution was diluted with dichloromethane, washed with 0.1 M HCl (50 mL × 3), saturated sodium bicarbonate (50 mL × 3), brine (50 mL × 3), dried over sodium sulfate, filtered and concentrated *in vacuo* to yield the monomer **CoumAAm** as a light orange solid. Yield: 1.62 g (97.6%). ^{1}H NMR (500 MHz, DMSO-d_6): δ (ppm) 8.38 (t, 1H), 7.68 (d, 1H), 7.01-6.95 (m, 2H), 6.32-6.06 (m, 3H), 5.63-5.58 (dd, 1H), 4.15 (t, 2H), 3.54 (dd, 2H), 2.39 (s, 3H). ^{13}C NMR (125 MHz, DMSO-d_6): δ (ppm) 164.94, 161.41, 160.11, 154.70, 153.35, 131.51, 126.47, 125.43, 113.23, 112.36, 111.23, 101.29, 66.98, 38.06, 18.11. ESI-HRMS: $[M+H]^+$ calcd. for $C_{15}H_{15}NO_4$, 274.1074; found, 274.1087.

Copolymerization of DMA and CoumAc (99:1)

In a typical copolymerization, DMA (2.00 g, 20.2 mmol), CoumAc (55.9 mg, 0.204 mmol), and AIBN (66.9 mg, 0.400 mmol, 0.02 equiv. relative to total monomer) were dissolved in 1,4-dioxane (12 mL, $[M]_o$ = 1.5 M) in a 20 mL scintillation vial and purged

with nitrogen. The vial was placed in a preheated heating block at 70 °C and after 1 h, the polymerization was quenched. The reaction mixture was dialyzed against deionized water and lyophilized to yield the final copolymer.

Copolymerization of DMA and CoumAAm (99:1)
In a typical copolymerization, DMA (2.00 g, 20.2 mmol), CoumAAm (55.7 mg, 0.204 mmol), and AIBN (66.9 mg, 0.400 mmol, 0.02 equiv. relative to total monomer) were dissolved in 1,4-dioxane (12 mL, $[M]_o$ = 1.5 M) in a 20 mL scintillation vial and purged with nitrogen. The vial was placed in a preheated heating block at 70 °C and after 1 h, the polymerization was quenched. The reaction mixture was dialyzed against deionized water and lyophilized to yield the final copolymer.

Copolymerization of DMA and CoumAc (95:5)
In a typical copolymerization, DMA (500 mg, 5.04 mmol), CoumAc (72.8 mg, 0.266 mmol), and AIBN (17.4 mg, 0.106 mmol, 0.02 equiv. relative to total monomer) were dissolved in 1,4-dioxane (10 mL, $[M]_o$ = 0.5 M) in a 20 mL scintillation vial and purged with nitrogen. The vial was placed in a preheated heating block at 60 °C and after 1 h, the polymerization was quenched. The reaction mixture was dialyzed against deionized water and lyophilized to yield the final copolymer.

Copolymerization of DMA and CoumAAm (95:5)
In a typical copolymerization, DMA (500 mg, 5.04 mmol), CoumAAm (72.5 mg, 0.265 mmol), and AIBN (17.4 mg, 0.106 mmol, 0.02 equiv. relative to total monomer) were dissolved in 1,4-dioxane (10 mL, $[M]_o$ = 0.5 M) in a 20 mL scintillation vial and purged with nitrogen. The vial was placed in a preheated heating block at 60 °C and after 1 h, the polymerization was quenched. The reaction mixture was dialyzed against deionized water and lyophilized to yield the final copolymer.

UV-Vis Dimerization Study
$PDMA_{0.95}$-*co*-$P(CoumAc)_{0.05}$ copolymer was dissolved in water (0.05 wt%) and subjected to long-wave UV irradiation (λ_{max} = 365 nm) for predetermined times (up to 4 h). The solution was characterized by UV-Vis spectroscopy as a function of irradiation time.

UV-Vis Retro-Dimerization Study
A solution of $PDMA_{0.95}$-*co*-$P(CoumAc)_{0.05}$ copolymer (0.05 wt% in water) that had been exposed to long-wave UV for 4 h was used for these measurements. The solution was exposed to short-wave UV (λ_{max} = 254 nm) for predetermined times (up to 15 min). The solution was characterized by UV-Vis spectroscopy as a function of irradiation time.

Gelation of Coumarin Copolymers
PDMA/Coumarin copolymers were dissolved in water at various weight percents, typically ~5-10 wt% for 5 mol% coumarin copolymers and ~10-30 wt% for 1 mol% coumarin copolymers. The solutions were irradiated with long-wave UV (λ_{max} = 365 nm) until gelation was complete (approx. 5-30 min).

Gel Reversal

Preformed hydrogels from PDMA/Coumarin copolymers were exposed to short-wave UV irradiation (λ_{max} = 254 nm). After approximately 30 min, the gel had reverted to the water-soluble prepolymer.

Formation of Hollow Tubes

3D printing was performed as described above. Prepolymer solutions were loaded into a glass syringe (Hamilton) with a 26 gauge blunt dispensing needle (McMaster Carr) before being printed into a jammed microgel support material (Ashland 980), prepared at 0.15 wt% and swollen at neutral pH. MATLAB scripts and trajectories were written such that the inner PDMA/coumarin cylinder [10 wt% P($DMA_{0.95}$-*co*-$CoumAc_{0.05}$)] was printed first, followed by the Nelfilcon A shell. After printing, tubes were cured using a 400 W, 320- to 390-nm UV flood curing lamp (Sunray) for 10 min. The cylinder was removed from the support medium by washing with water, and the cylinder was submerged in deionized water in a Petri dish. The sample was exposed to 254 nm light for 3 h and soaked in deionized water overnight to ensure complete removal of soluble coumarin copolymer. See Supporting Information Movie S1 for an example time-lapse video of this process. In this video, red and green insoluble fluorescent beads are added to the polymeric inks to add contrast. The printed materials shown in this video are not cured and are used solely to demonstrate the procedure for printing complex hydrogel structures.

Formation of Hollow Spheres

3D printing was performed as described above. Prepolymer solutions were loaded into a glass syringe (Hamilton) with a 26 gauge blunt dispensing needle (McMaster Carr) before being printed into a jammed microgel support material (Ashland 980), prepared at 0.15 wt% and swollen at neutral pH. MATLAB scripts and trajectories were written such that the lower portion of the Nelfilcon A shell was printed first, followed by the interior coumarin [30 wt% P($DMA_{0.99}$-*co*-$CoumAc_{0.01}$)] sphere, and finally the upper portion of the Nelfilcon A shell. After printing, spheres were cured using a 400 W, 320- to 390-nm UV flood curing lamp (Sunray) for 10 min. The sphere was removed from the support medium by washing with water, and submerged in deionized water in a Petri dish. The sample was exposed to 254 nm light for 3 h and soaked in deionized water overnight to ensure complete removal of soluble coumarin copolymer. See Supporting Information Movie S3 for an example time-lapse video of this process. In this video, green insoluble fluorescent beads are added to the polymeric inks to add contrast. The printed materials shown in this video are not cured and are used solely to demonstrate the procedure for printing complex hydrogel structures.

Supplemental Figures

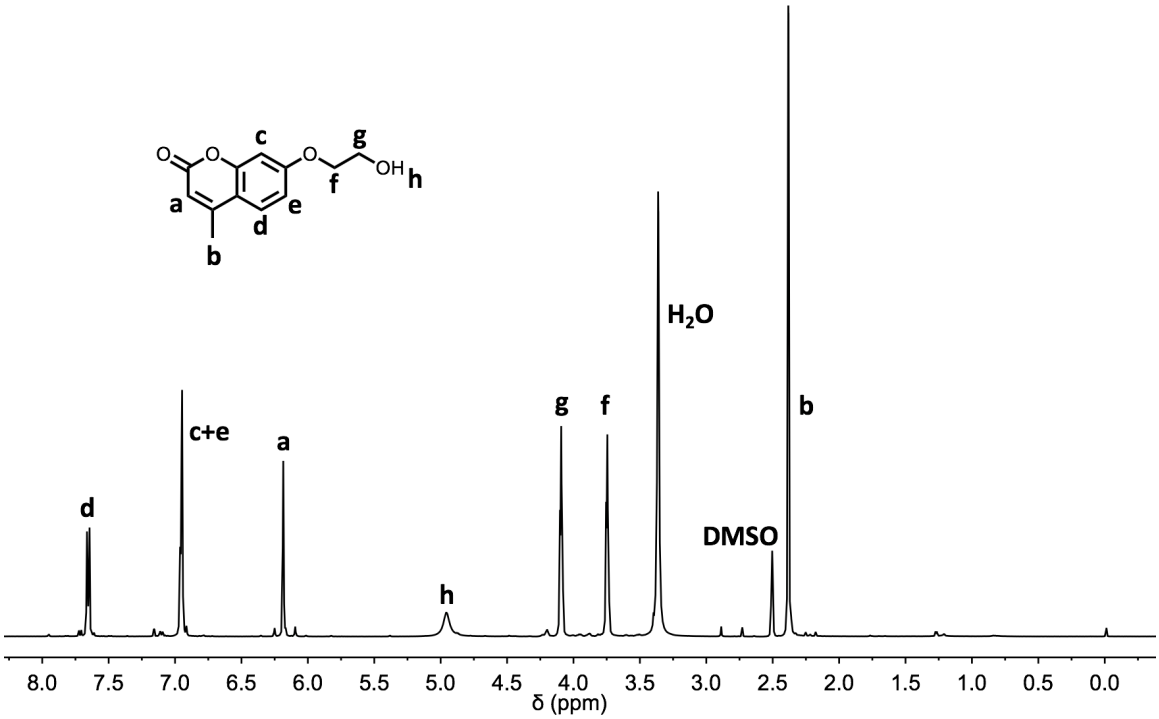

Figure S1. ^{1}H NMR spectrum of 7-(2-hydroxyethoxy)-4-methylcoumarin (500 MHz, DMSO-d_6)

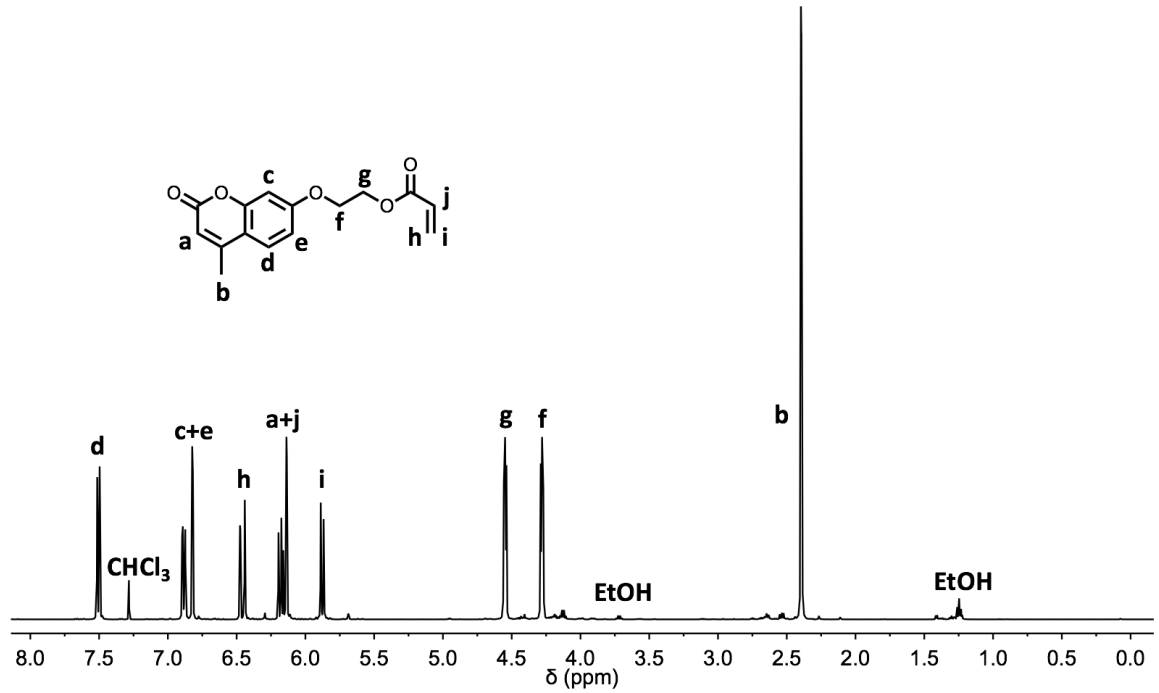

Figure S2. ^{1}H NMR spectrum of CoumAc (500 MHz, $CDCl_3$)

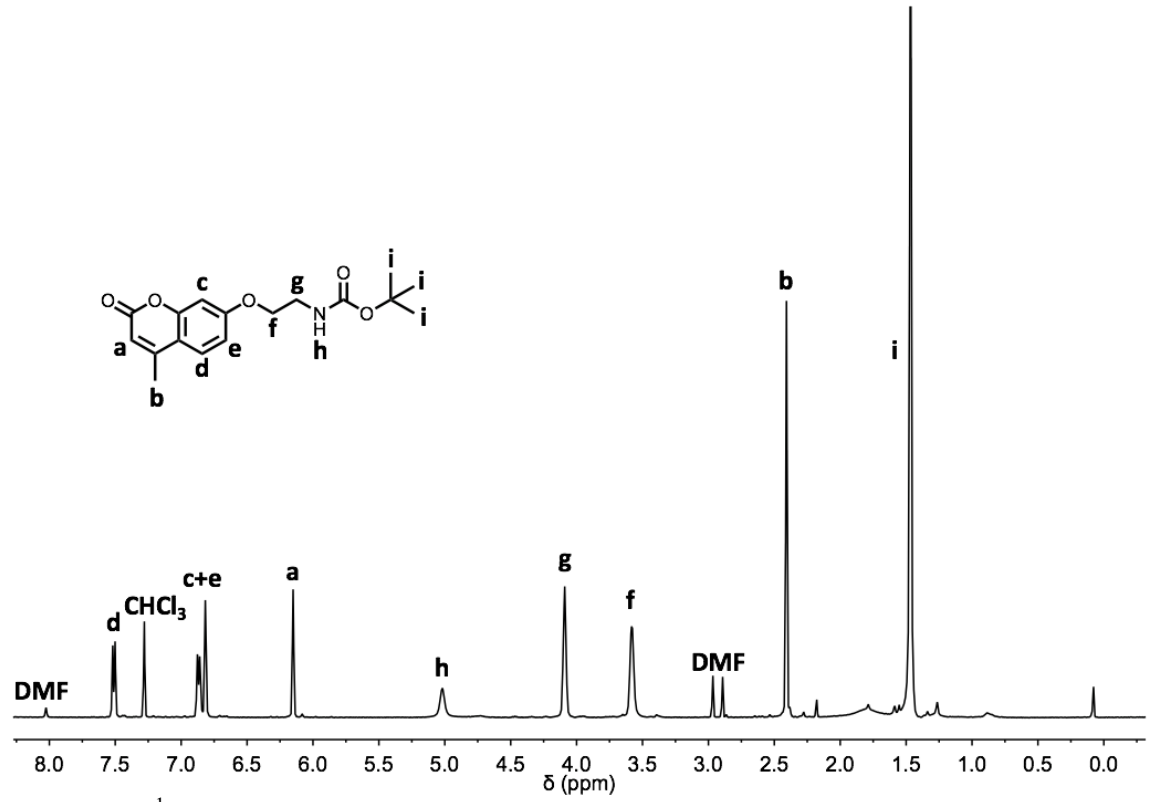

Figure S3. ^{1}H NMR spectrum of 7-(2-*boc*-aminoethoxy)-4-methylcoumarin (500 MHz, $CDCl_3$)

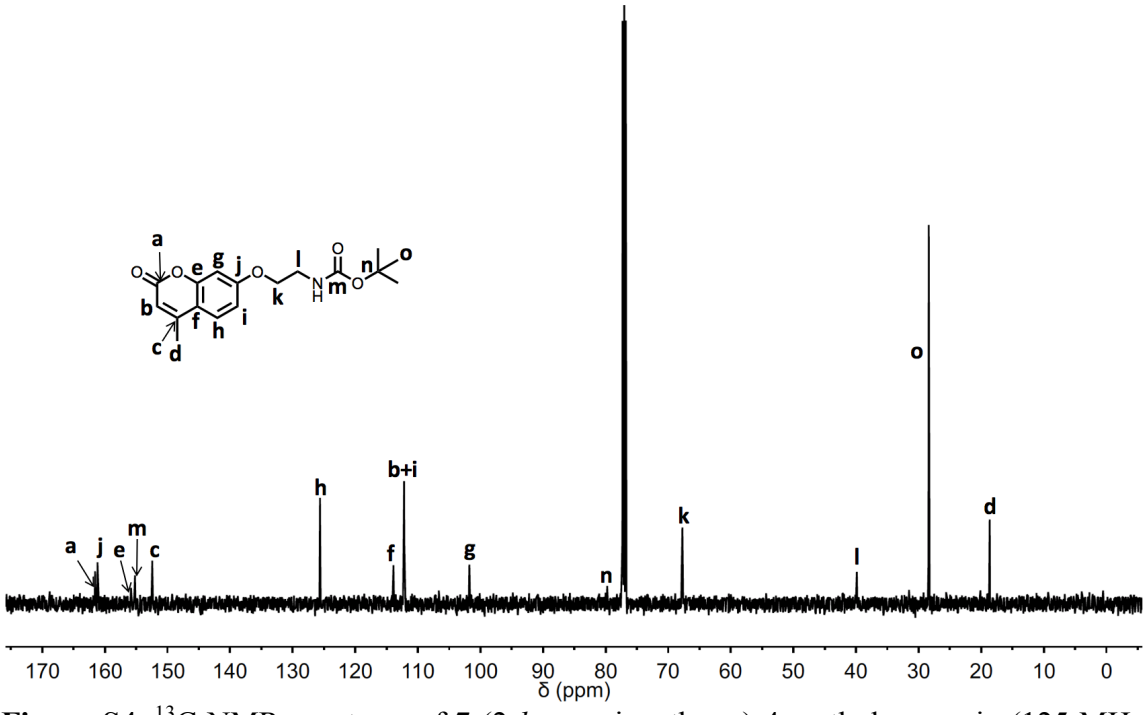

Figure S4. ^{13}C NMR spectrum of 7-(2-*boc*-aminoethoxy)-4-methylcoumarin (125 MHz, $CDCl_3$)

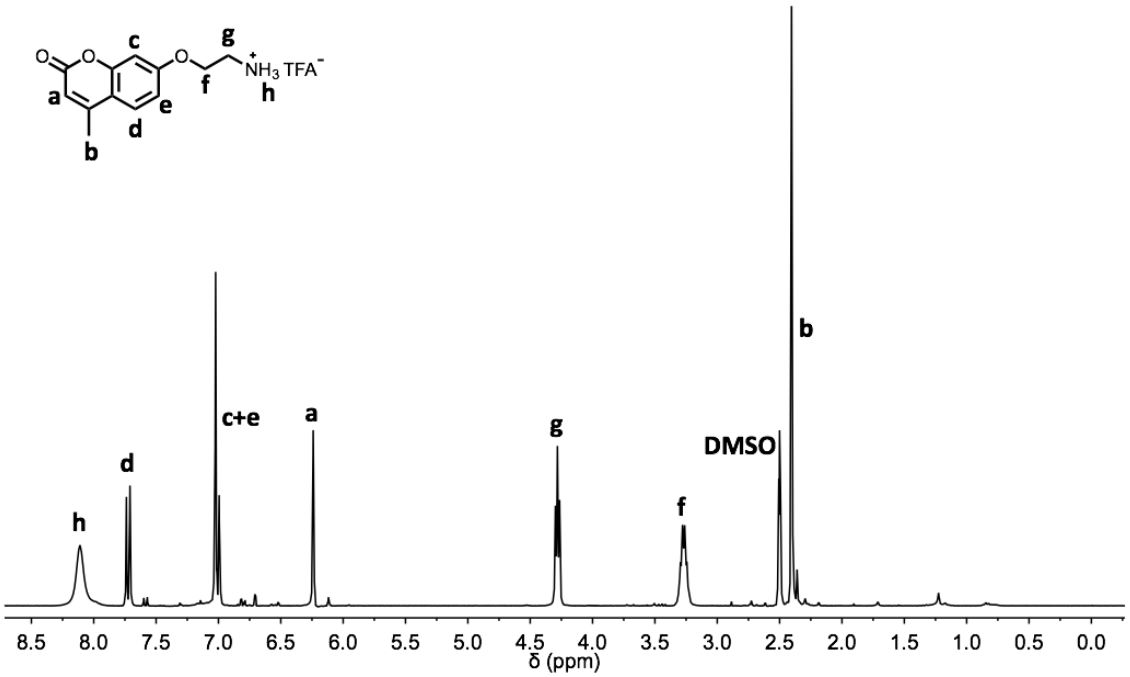

Figure S5. ^{1}H NMR spectrum of 7-(2-(ammonium trifluoroacetate)ethoxy)-4-methylcoumarin (500 MHz, DMSO-d_6)

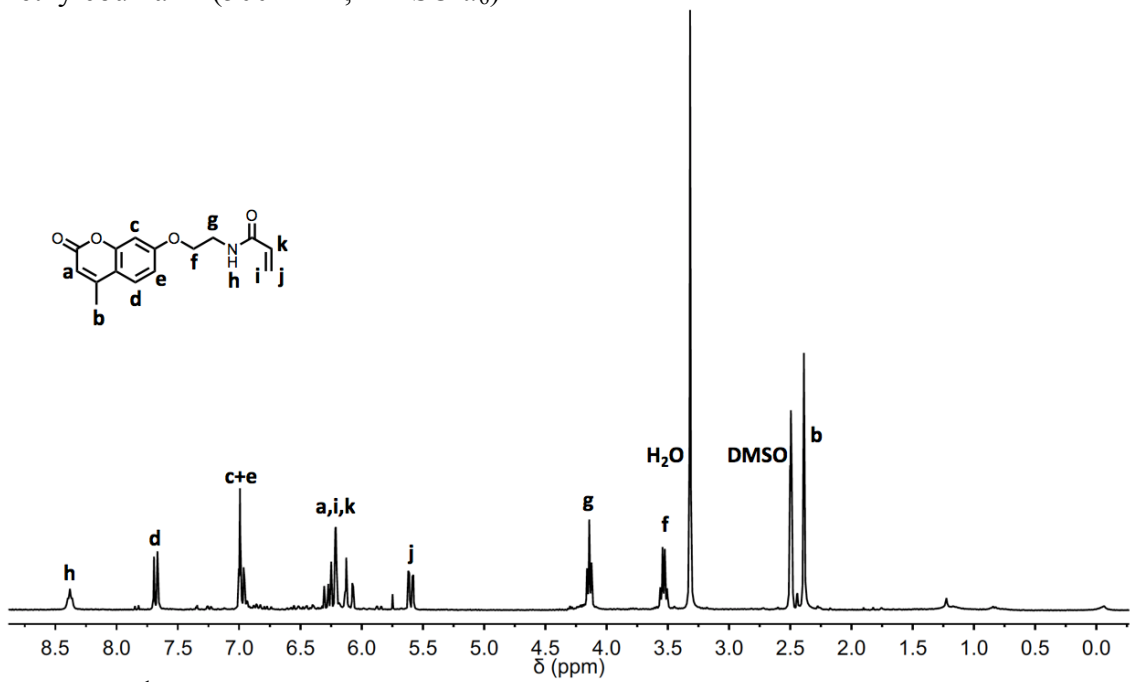

Figure S6. ^{1}H NMR spectrum of CoumAAm (500 MHz, DMSO-d_6)

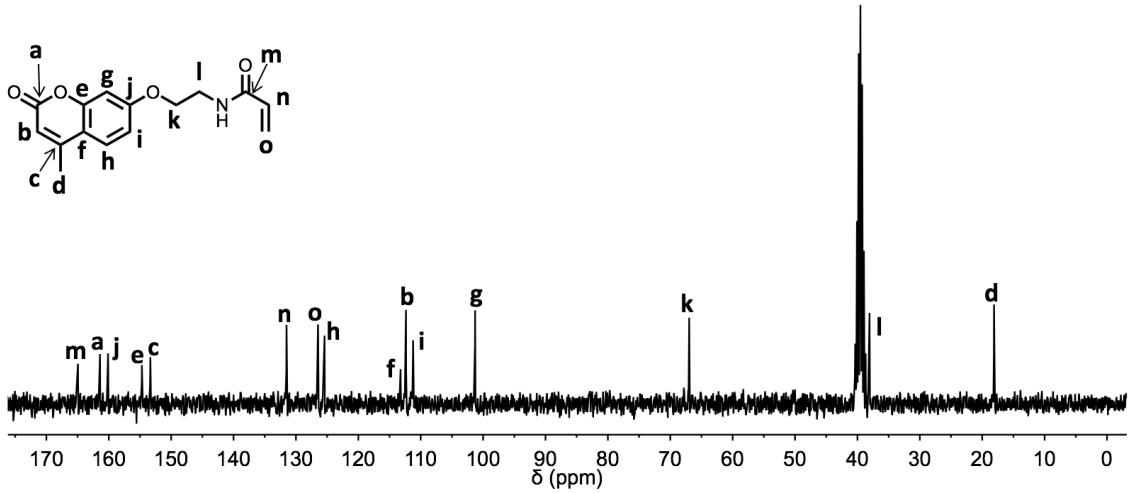

Figure S7. ^{13}C NMR spectrum of CoumAAm (125 MHz, DMSO-d_6)

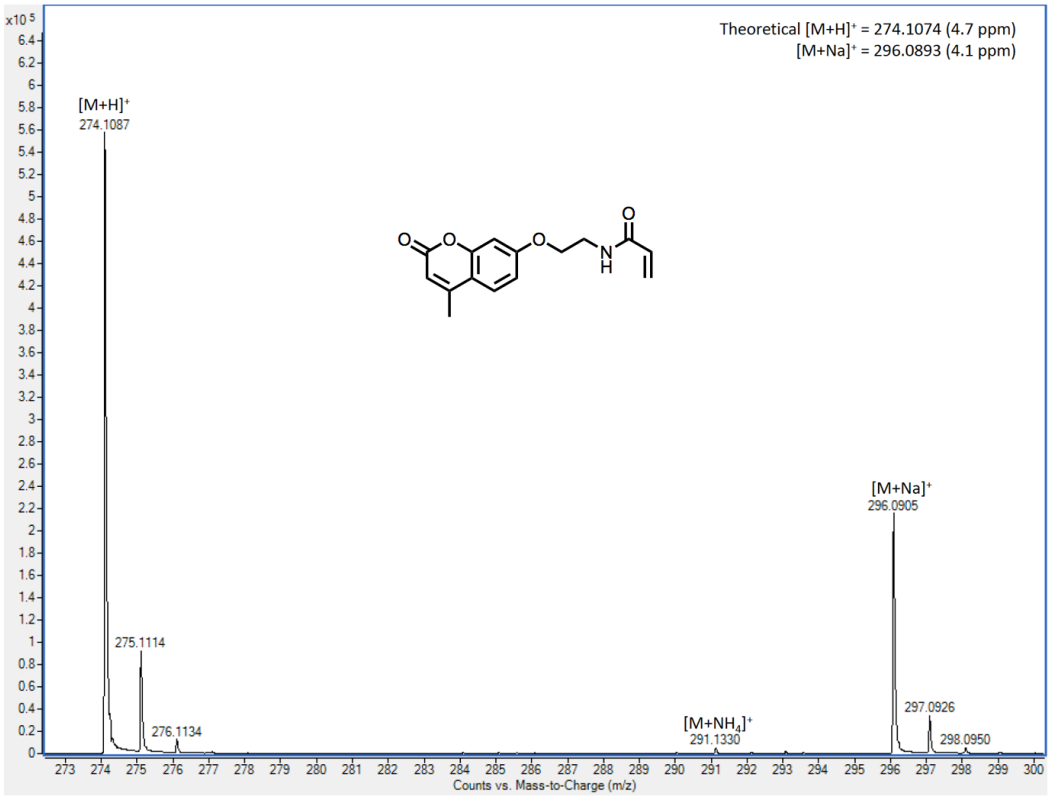

Figure S8. High-resolution mass spectrum of CoumAAm

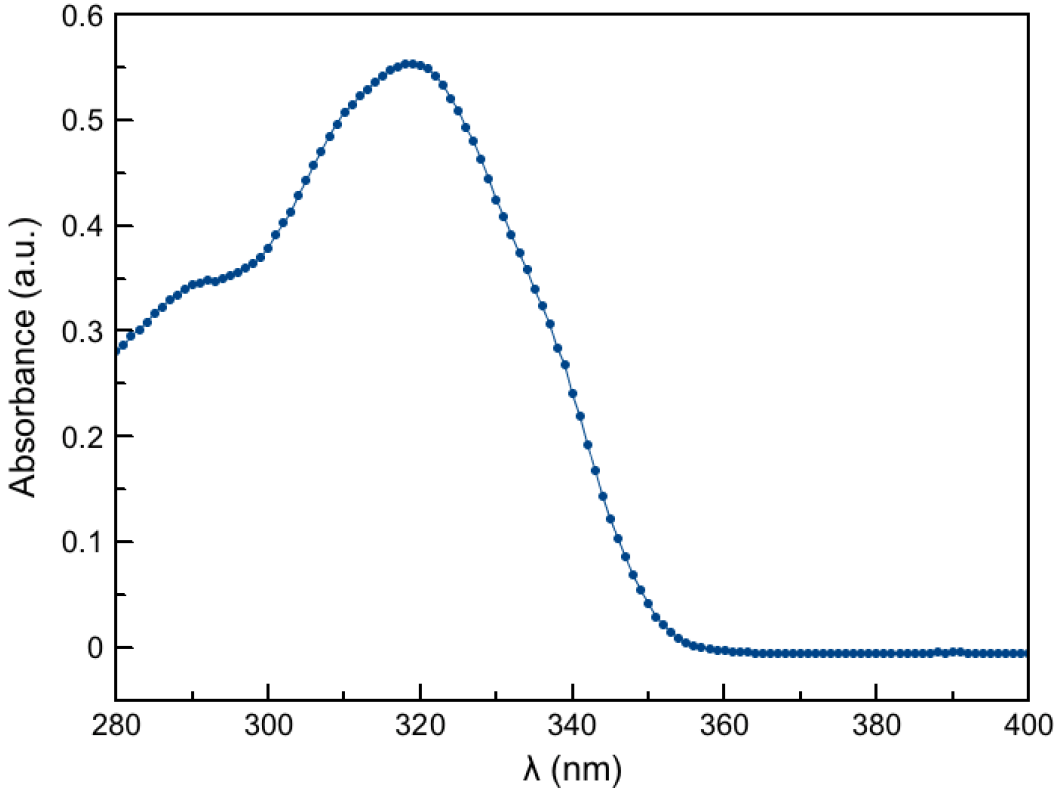

Figure S9. UV-vis absorption spectrum of CoumAc

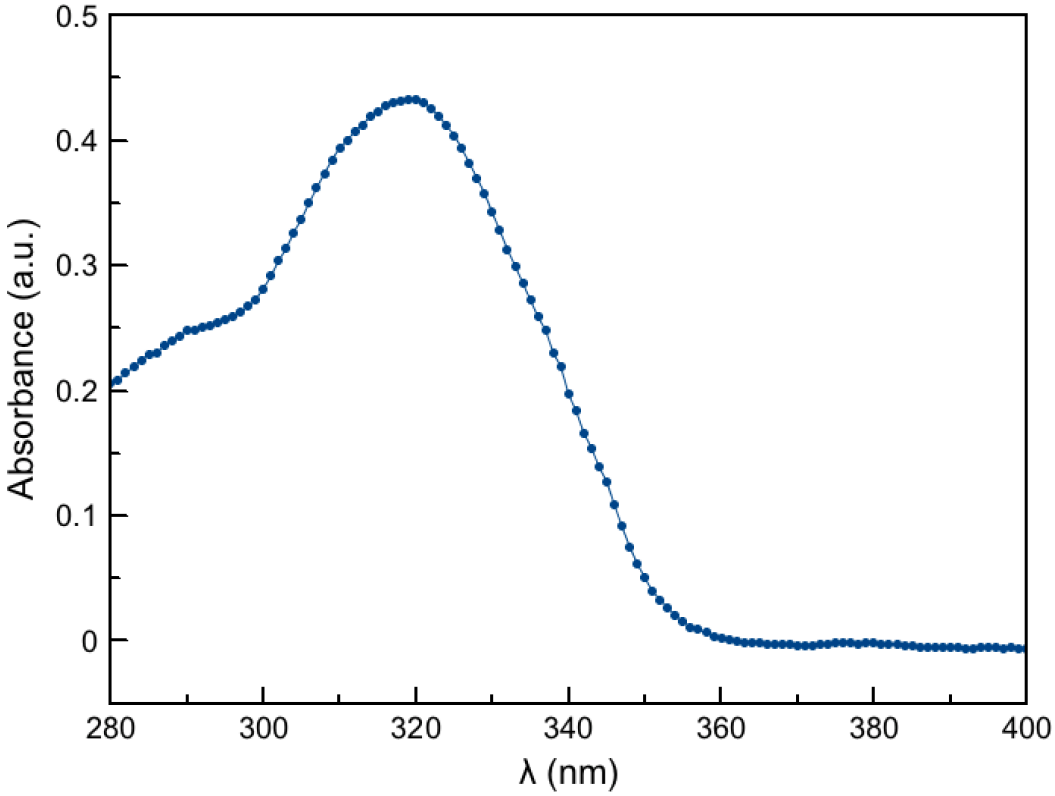

Figure S10. UV-vis absorption spectrum of CoumAAm

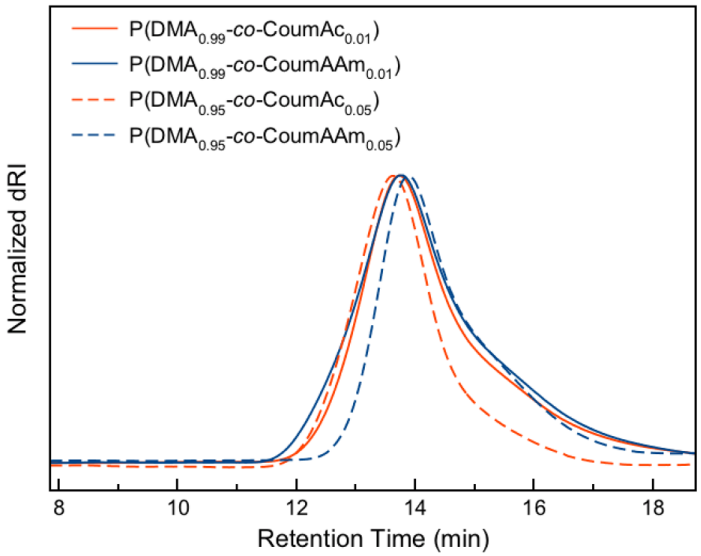

Figure S11. Gel permeation chromatograms of PDMA/Coumarin copolymers with differential refractive index (dRI) detection

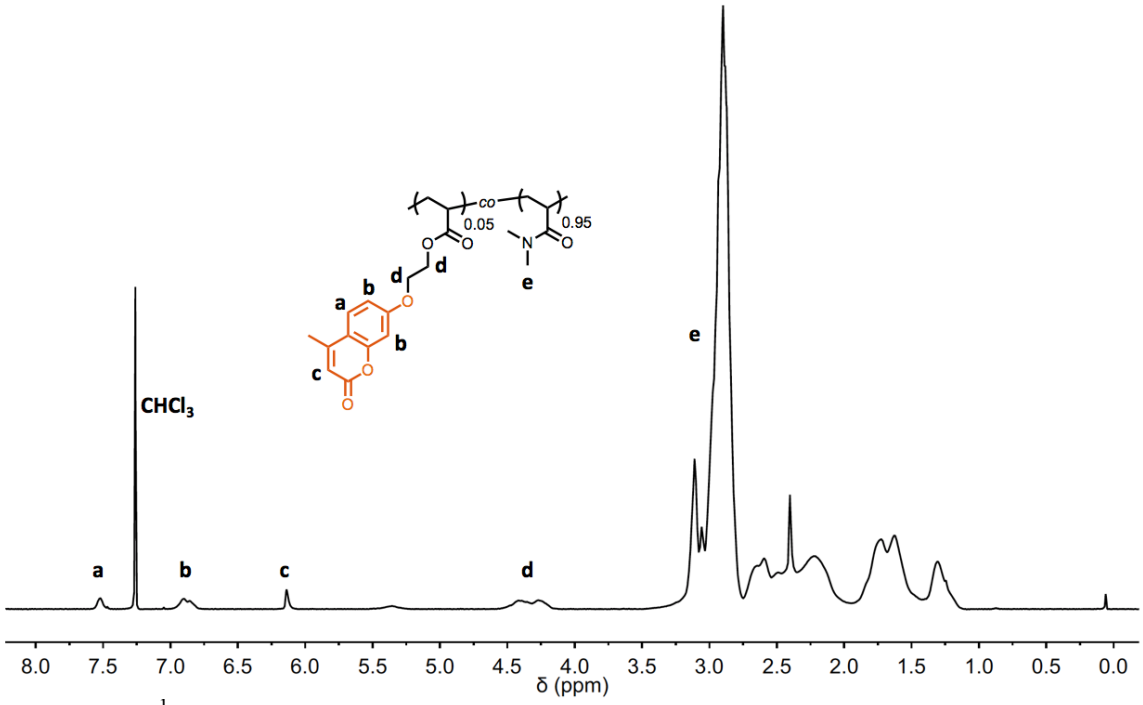

Figure S12. ^{1}H NMR spectrum of P($DMA_{0.95}$-*co*-$CoumAc_{0.05}$) (500 MHz, $CDCl_3$)

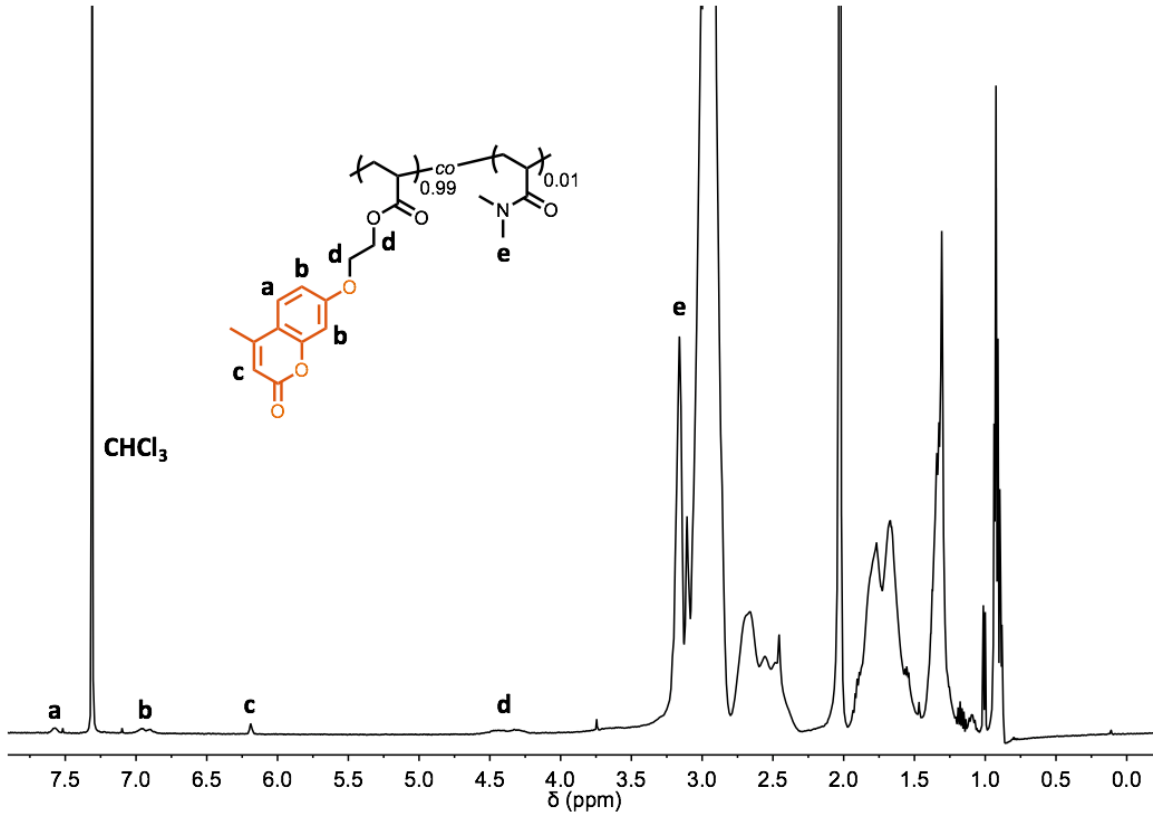

Figure S13. ^{1}H NMR spectrum of P(DMA$_{0.99}$-*co*-CoumAc$_{0.01}$) (500 MHz, $CDCl_3$)

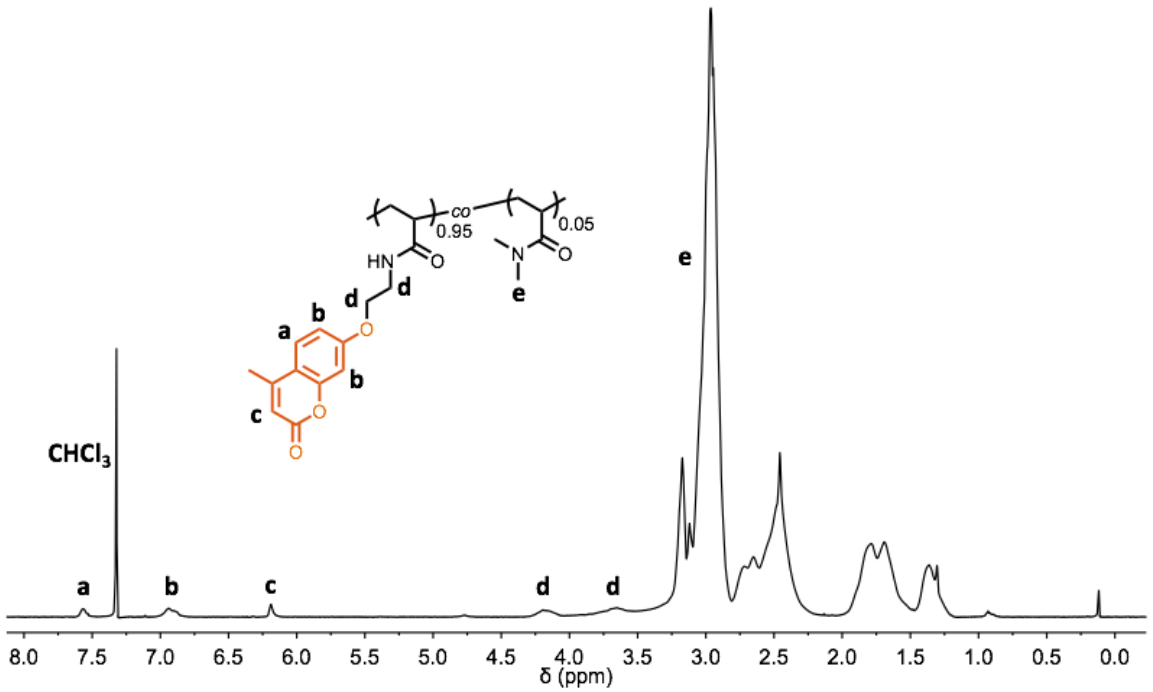

Figure S14. ^{1}H NMR spectrum of P(DMA$_{0.95}$-*co*-CoumAAm$_{0.05}$) (500 MHz, $CDCl_3$)

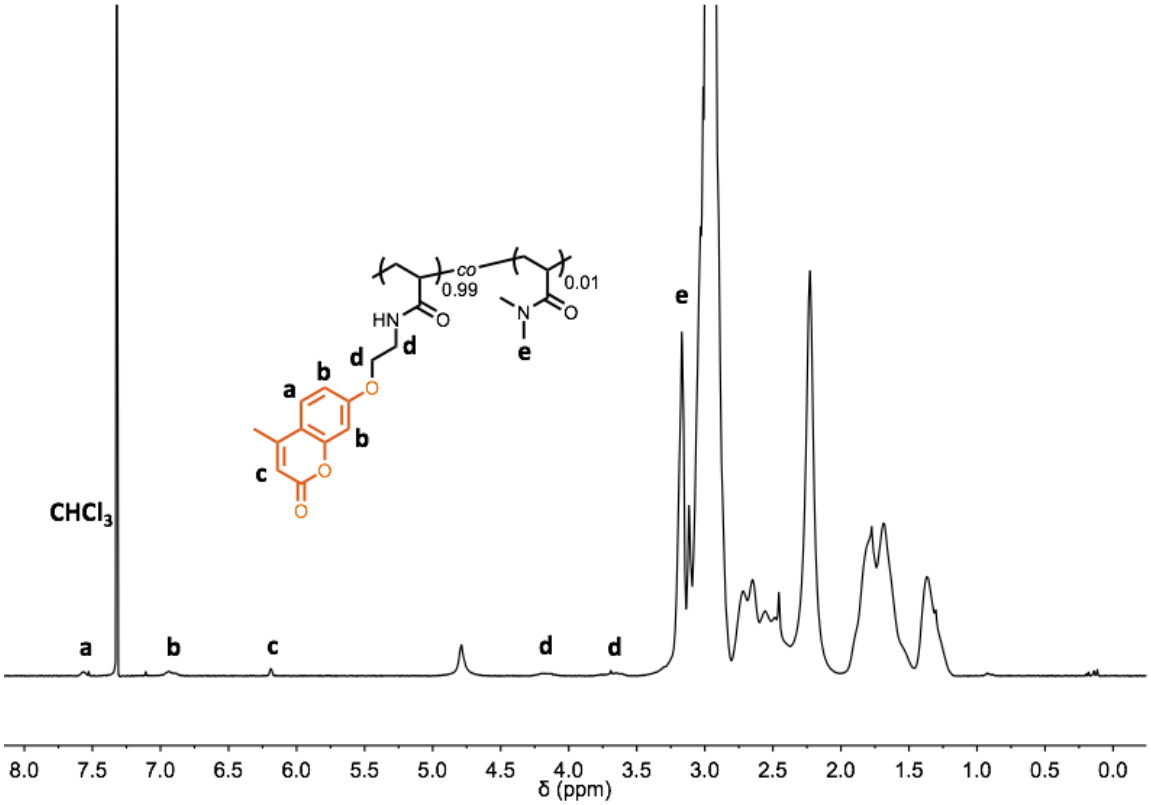

Figure S15. ^{1}H NMR spectrum of P(DMA$_{0.99}$-*co*-CoumAAm$_{0.01}$) (500 MHz, $CDCl_3$)

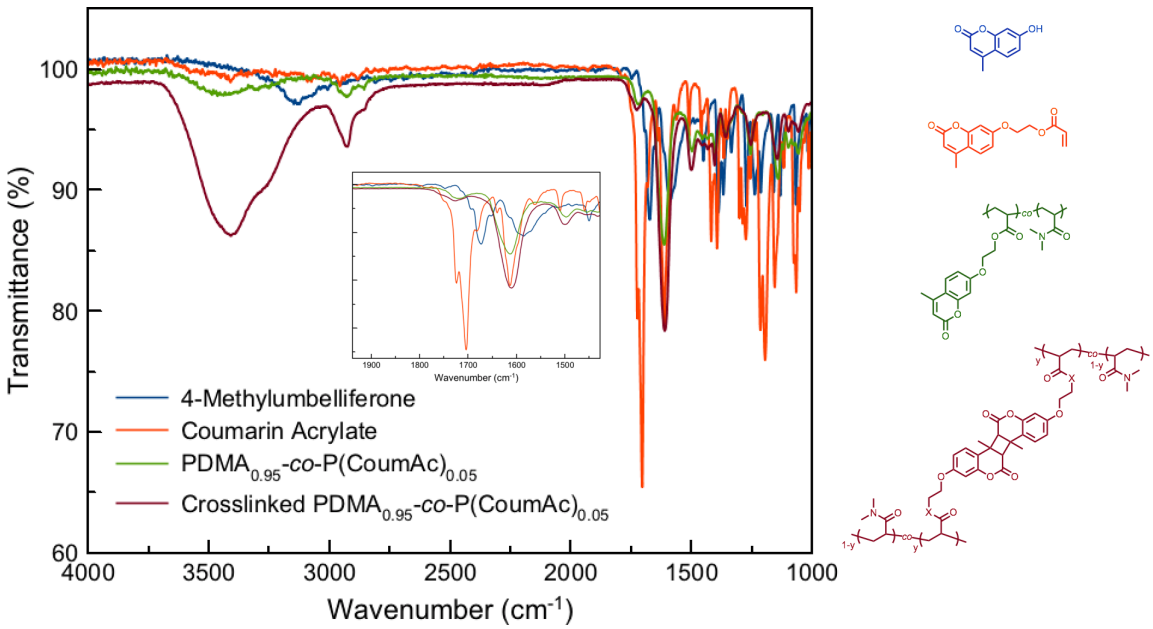

Figure S16. FTIR spectra of 4-methylumbelliferone (blue), CoumAc (orange), PDMA$_{0.95}$-*co*-P(CoumAc)$_{0.05}$ (green), and crosslinked PDMA$_{0.95}$-*co*-P(CoumAc)$_{0.05}$ (maroon)

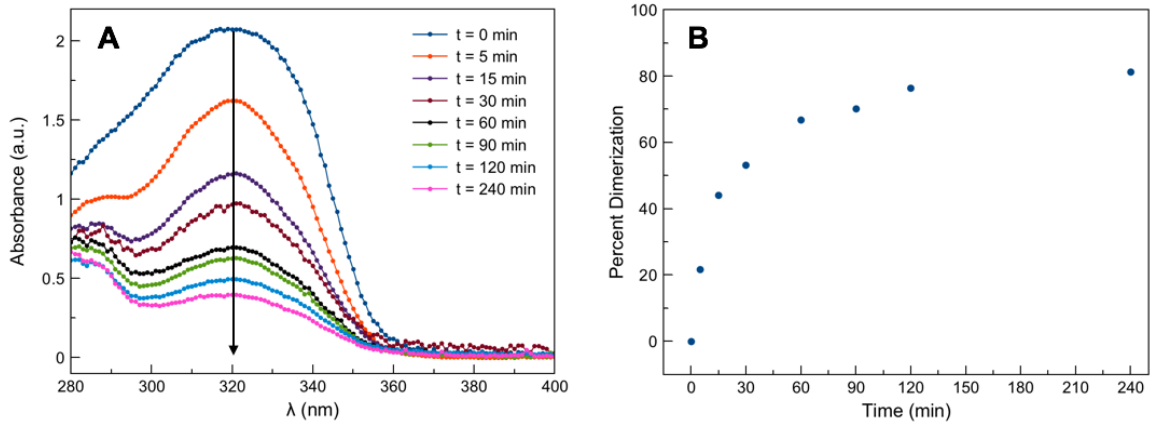

Figure S17. (A) UV-Vis spectra of P(DMA$_{0.95}$-*co*-CoumAAm$_{0.05}$) copolymer (0.05 wt% in water) as a function of irradiation time with long-wave UV (λ_{max} = 365 nm). (B) Percent coumarin dimerization as a function of irradiation time at 365 nm.

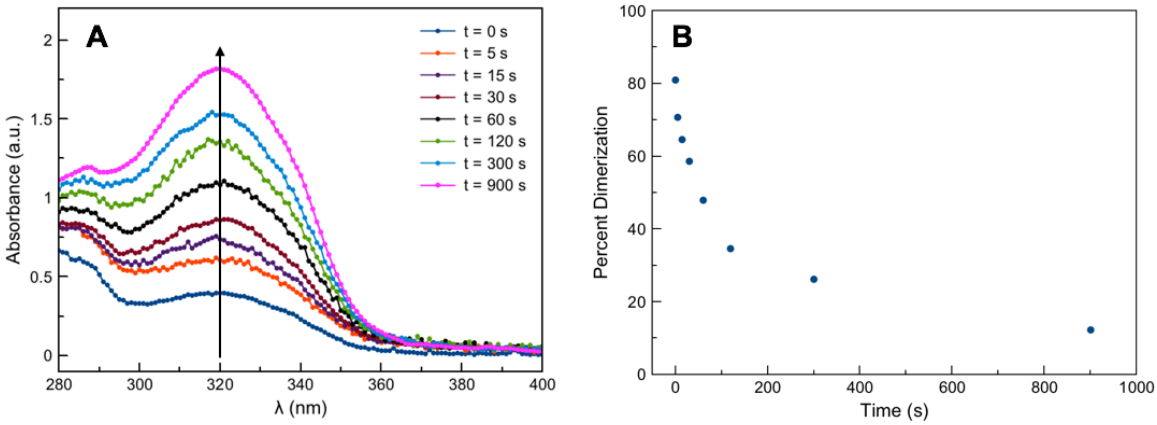

Figure S18. (A) After 4 h irradiation at 365 nm, the solution was irradiated with short-wave UV (λ_{max} = 254 nm). UV-Vis spectra of P(DMA$_{0.95}$-*co*-CoumAAm$_{0.05}$) copolymer (0.05 wt% in water) as a function of irradiation time with short-wave UV (λ_{max} = 254 nm). (B) Percent coumarin de-dimerization as a function of irradiation time at 254 nm.

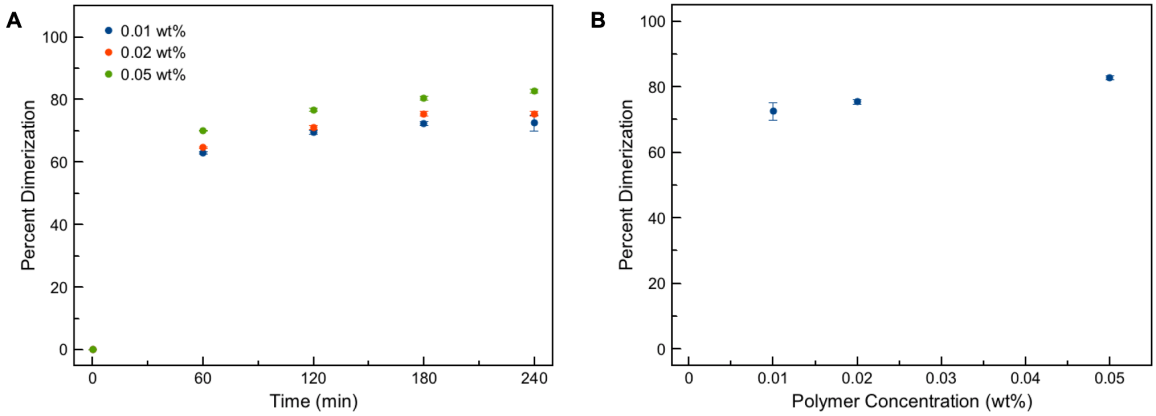

Figure S19. (A) Dimerization kinetics of P(DMA$_{0.95}$-*co*-CoumAc$_{0.05}$) at polymer concentrations of 0.01, 0.02, and 0.05 wt%. (B) Percent dimerization of P(DMA$_{0.95}$-*co*-CoumAc$_{0.05}$) after 4 h of irradiation with 365 nm light as a function of polymer concentration.

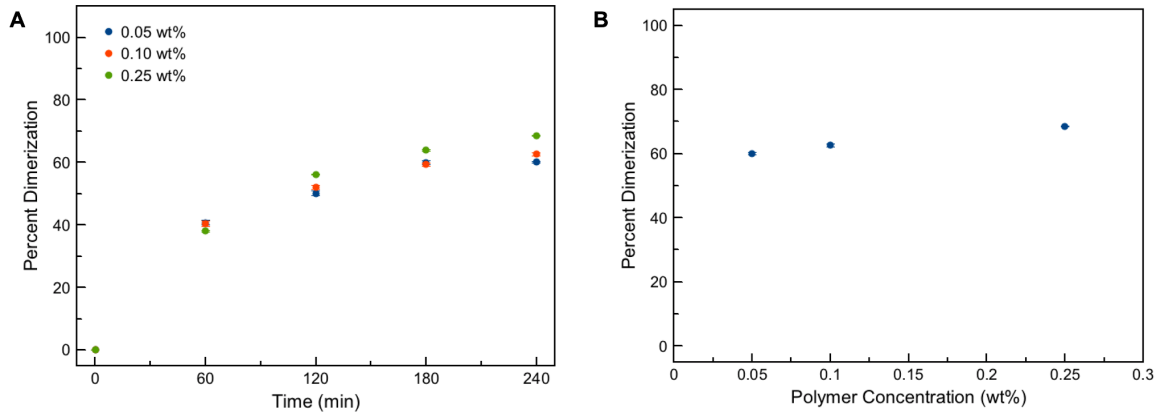

Figure S20. (A) Dimerization kinetics of P($DMA_{0.99}$-*co*-$CoumAc_{0.01}$) at polymer concentrations of 0.05, 0.10, and 0.25 wt%. (B) Percent dimerization of P($DMA_{0.99}$-*co*-$CoumAc_{0.01}$) after 4 h of irradiation with 365 nm light as a function of polymer concentration.

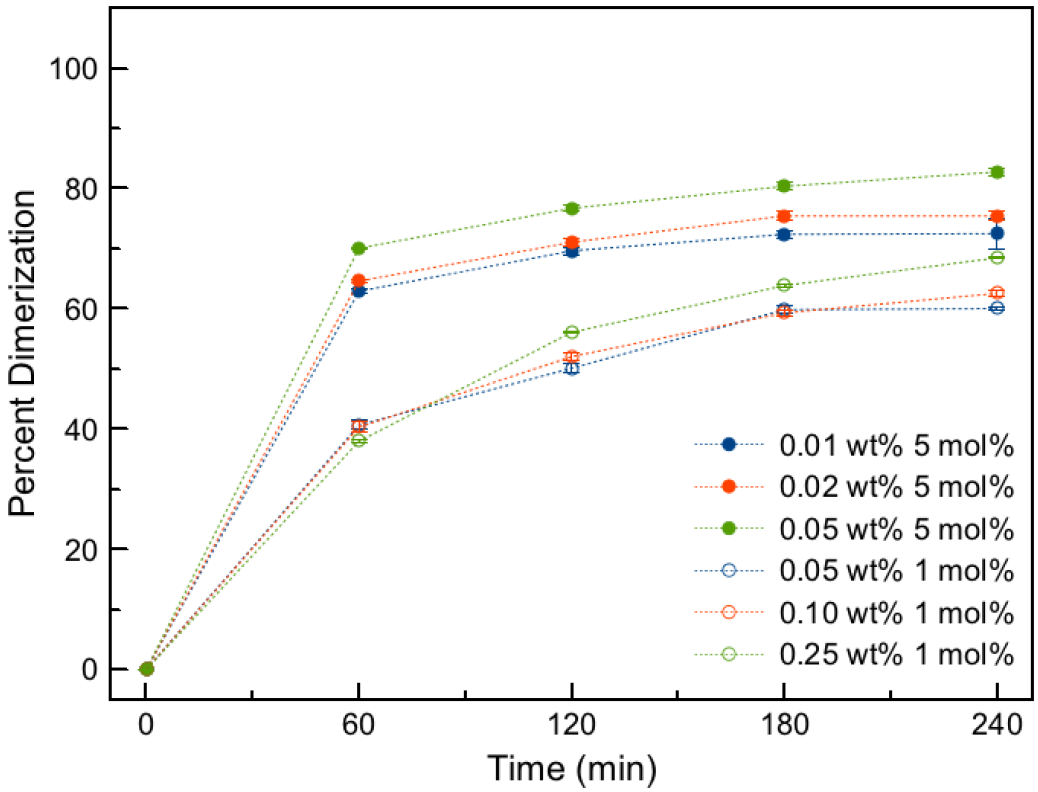

Figure S21. Comparison of dimerization kinetics of P($DMA_{0.99}$-*co*-$CoumAc_{0.01}$) at polymer concentrations of 0.05, 0.10, and 0.25 wt% and P($DMA_{0.99}$-*co*-$CoumAc_{0.01}$) at polymer concentrations of 0.05, 0.10, and 0.25 wt%.

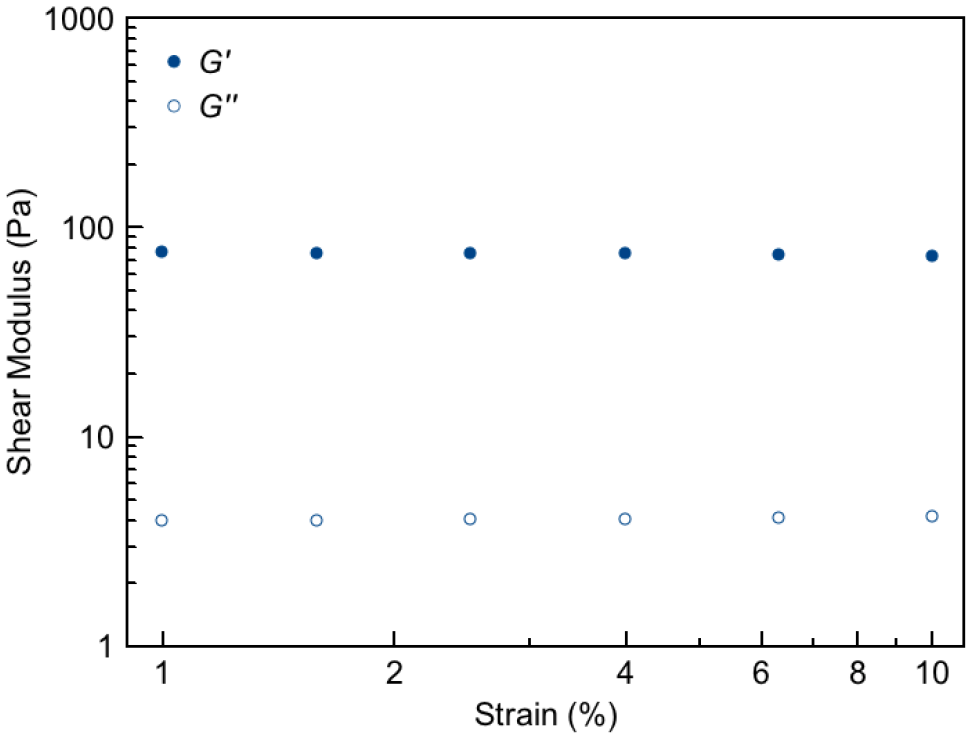

Figure S22. Representative strain sweep of a 5 wt% hydrogel of P(DMA$_{0.95}$-*co*-CoumAc$_{0.05}$).

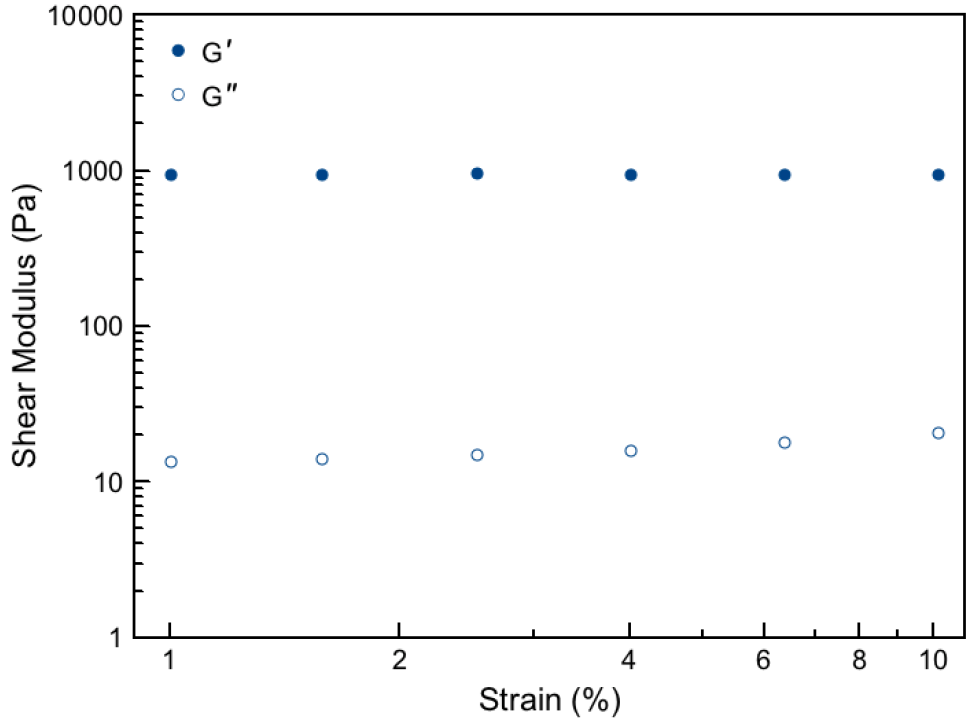

Figure S23. Representative strain sweep of a 10 wt% hydrogel of P(DMA$_{0.95}$-*co*-CoumAc$_{0.05}$).

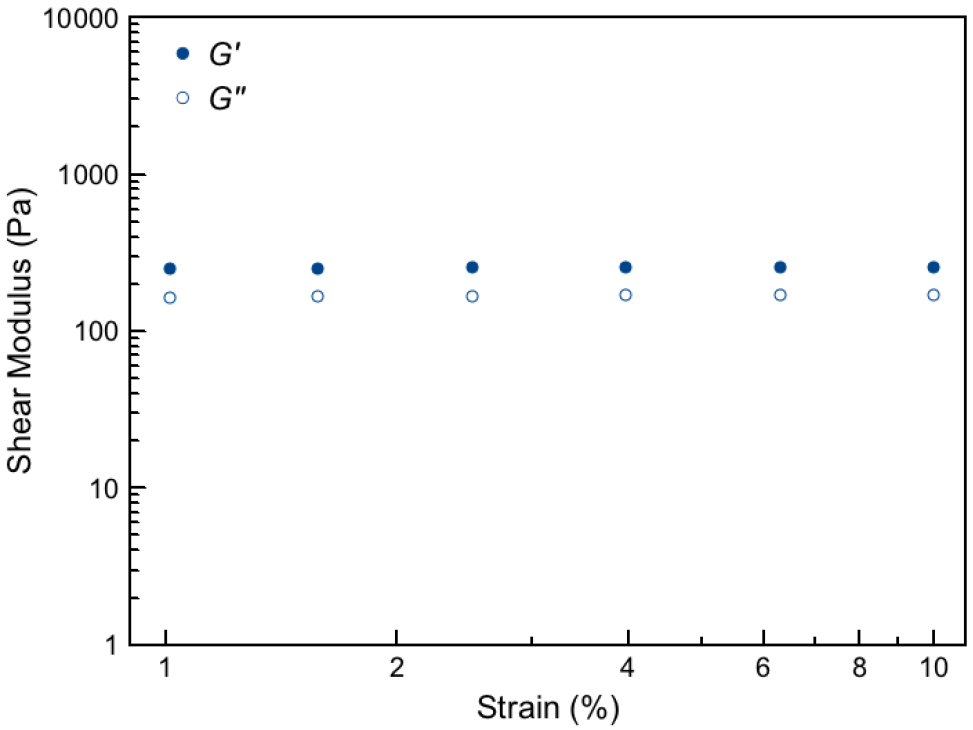

Figure S24. Representative strain sweep of a 20 wt% hydrogel of P(DMA$_{0.99}$-*co*-CoumAc$_{0.01}$).

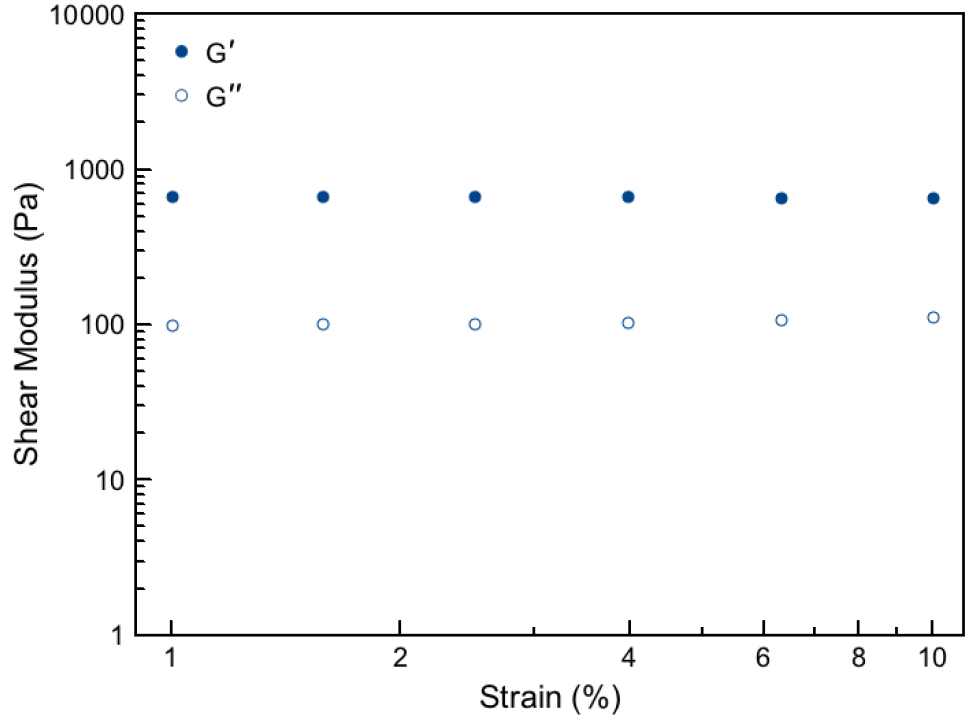

Figure S25. Representative strain sweep of a 30 wt% hydrogel of P(DMA$_{0.99}$-*co*-CoumAc$_{0.01}$).

Table S1. Storage (G′) and loss (G″) moduli of hydrogels formed from P(DMA$_{0.95}$-*co*-CoumAc$_{0.05}$) and P(DMA$_{0.99}$-*co*-CoumAc$_{0.01}$) measured at 1% strain and an angular frequency of 10 rad s^{-1}

Polymer	Concentration (wt%)	G′ (Pa)	G″ (Pa)
P(DMA$_{0.95}$-*co*-CoumAc$_{0.05}$)	5	76 ± 26	6 ± 2
P(DMA$_{0.95}$-*co*-CoumAc$_{0.05}$)	10	827 ± 114	27 ± 13
P(DMA$_{0.99}$-*co*-CoumAc$_{0.01}$)	20	187 ± 87	120 ± 49
P(DMA$_{0.99}$-*co*-CoumAc$_{0.01}$)	30	577 ± 84	164 ± 66

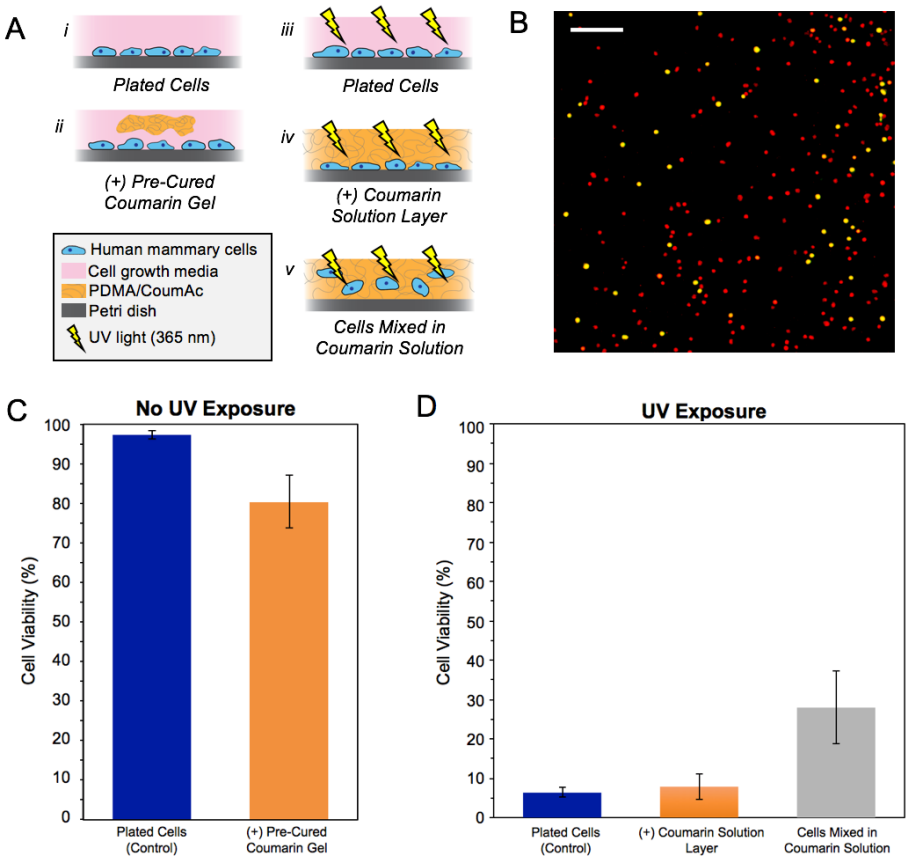

Figure S26. Cell viability of MCF-10A (human mammary epithelial cells). (A) Pictorial representations of the conditions in this study; (*i*) control in the absence of long-wave UV irradiation; (*ii*) plated cells with a slab of pre-cured coumarin gel introduced into the dish; (*iii*) control in the presence of long-wave UV irradiation; (*iv*) cells were plated, then a solution of coumarin copolymer was introduced and cured under long-wave UV irradiation; (*v*) cells were premixed in a solution containing coumarin copolymer and cured under long-wave UV irradiation. (B) A sample live-dead assay; all cells are stained red, and dead cells are stained green. The overlay results in dead cells appearing yellow-orange. (C) Cell viability under conditions (*i*) and (*ii*) in the absence of long-wave UV irradiation. (D) Cell viability under conditions (*iii*), (*iv*), and (*v*) in the presence of long-wave UV irradiation.

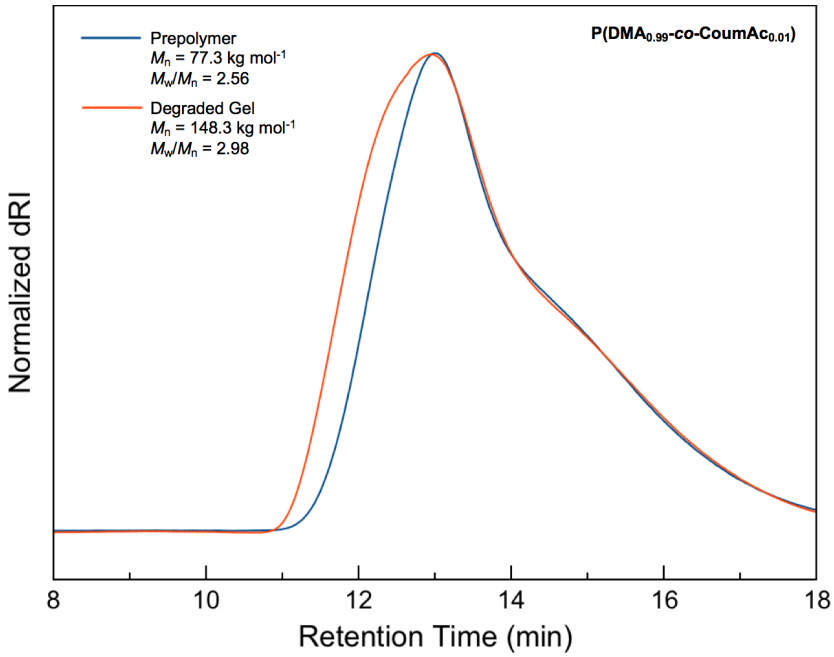

Figure S27. GPC analysis of degraded 10 wt% P(DMA$_{0.99}$-*co*-CoumAc$_{0.01}$) hydrogel indicates the presence of lightly branched polymers due to incomplete cycloreversion.

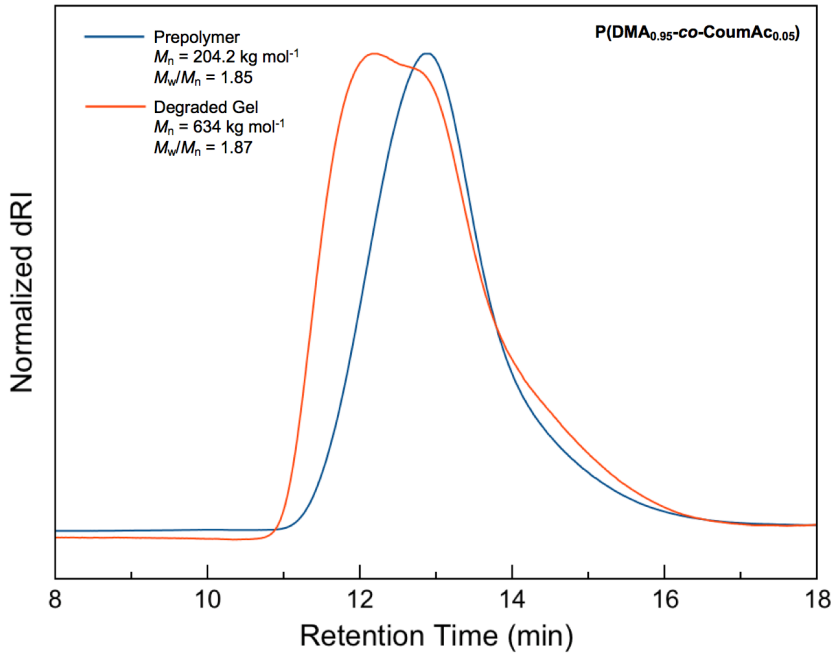

Figure S28. GPC analysis of degraded 5 wt% P(DMA$_{0.95}$-*co*-CoumAc$_{0.05}$) hydrogel indicates the presence of lightly branched polymers due to incomplete cycloreversion.

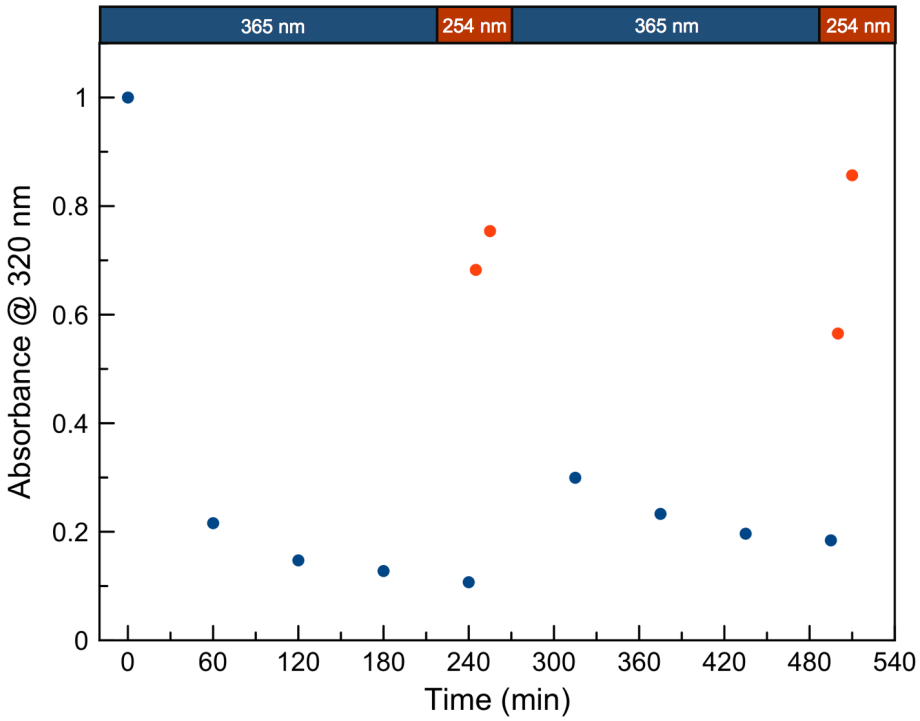

Figure S29. Dimerization and retro-dimerization cycles of P(DMA$_{0.95}$-*co*-CoumAc$_{0.05}$) in water (0.05 wt% polymer). After 240 min of irradiation with 365 nm light, nearly 90% of coumarin units have dimerized. Irradiation with 254 nm light for 15 min recovers ~80% of the absorbance at 320 nm attributed to the coumarin monomer. Similar results are obtained through a second cycle of dimerization and monomer formation.

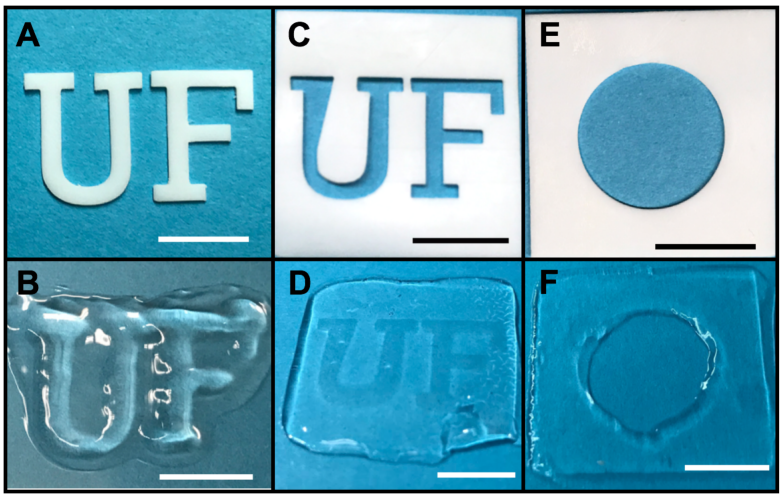

Figure S30. Results of photoetching using photomasked hydrogels under irradiation with short-wave UV. Scale bars are 1 cm. (A) UF positive mask; (B) A raised "UF" remains after masking with the UF positive mask; (C) UF negative mask; (D) An indented "UF" is imprinted into the gel after masking with the UF negative mask; (E) Circle negative mask; (F) An indented circle is imprinted into the gel after masking with the circle negative mask.

References

1. Bhattacharjee, T.; Zehnder, S. M.; Rowe, K. G.; Jain, S.; Nixon, R. M.; Sawyer, W. G.; Angelini, T. E., Writing in the Granular Gel Medium. *Sci. Adv.* **2015,** *1*, e1500655.
2. Shaughnessy, K. H.; Kim, P.; Hartwig, J. F., A Fluorescence-Based Assay for High-Throughput Screening of Coupling Reactions. Application to Heck Chemistry. *J. Am. Chem. Soc.* **1999,** *121*, 2123-2132.
3. Ling, J.; Rong, M. Z.; Zhang, M. Q., Coumarin Imparts Repeatable Photochemical Remendability to Polyurethane. *J. Mater. Chem.* **2011,** *21*, 18373-18380.
4. Onbulak, S.; Rzayev, J., Cylindrical Nanocapsules from Photo-Crosslinkable Core-Shell Bottlebrush Copolymers. *Polym. Chem.* **2015,** *6*, 764-771.
5. Jiang, J.; Qi, B.; Lepage, M.; Zhao, Y., Polymer Micelles Stabilization on Demand through Reversible Photo-Cross-Linking *Macromolecules* **2007,** *40*, 790-792.
6. Chauhan, K.; Datta, A.; Adhikari, A.; Chuttani, K.; Kumar Singh, A.; Mishra, A. K., ^{68}Ga Based Probe for Alzeheimer's Disease: Synthesis and Preclinical Evaluation of Homodimeric Chalcone in β-Amyloid Imaging. *Org. Biomol. Chem.* **2014,** *12*, 7328-7337.